Q-SWITCHED RAMAN FIBER LASER BASED ON 2D MATERIALS AS SATURABLE ABSORBER

NAJWA BINTI HISAMUDDIN

FACULTY OF SCIENCE
UNIVERSITY OF MALAYA
KUALA LUMPUR

2018

Q-SWITCHED RAMAN FIBER LASER BASED ON 2D MATERIALS AS SATURABLE ABSORBER

NAJWA BINTI HISAMUDDIN

DISSERTATION SUBMITTED IN FULFILLMENT OF THE REQUIREMENT FOR THE DEGREE OF MASTER OF SCIENCE

DEPARTMENT OF PHYSICS
FACULTY OF SCIENCE
UNIVERSITY OF MALAYA
KUALA LUMPUR

2018

UNIVERSITY OF MALAYA
ORIGINAL LITERARY WORK DECLARATION

Name of Candidate: **NAJWA BINTI HISAMUDDIN**

Matric No: **SGR150014**

Name of Degree: **MASTER OF SCIENCE**

Title of Project Paper/Research Report/Dissertation/Thesis ("this Work"):

Q-SWITCHED RAMAN FIBER LASER BASED ON 2D MATERIALS AS SATURABLE ABSORBER

Field of Study: **EXPERIMENTAL PHYSICS**

I do solemnly and sincerely declare that:

(1) I am the sole author/writer of this Work;
(2) This Work is original;
(3) Any use of any work in which copyright exists was done by way of fair dealing and for permitted purposes and any excerpt or extract from, or reference to or reproduction of any copyright work has been disclosed expressly and sufficiently and the title of the Work and its authorship have been acknowledged in this Work;
(4) I do not have any actual knowledge nor do I ought reasonably to know that the making of this work constitutes an infringement of any copyright work;
(5) I hereby assign all and every rights in the copyright to this Work to the University of Malaya ("UM"), who henceforth shall be owner of the copyright in this Work and that any reproduction or use in any form or by any means whatsoever is prohibited without the written consent of UM having been first had and obtained;
(6) I am fully aware that if in the course of making this Work I have infringed any copyright whether intentionally or otherwise, I may be subject to legal action or any other action as may be determined by UM.

Candidate's Signature Date:

Subscribed and solemnly declared before,

Witness's Signature Date:

Name:

Designation:

Q-SWITCHED RAMAN FIBER LASER BASED ON 2D MATERIALS AS SATURABLE ABSORBER

ABSTRACT

This thesis aims to demonstrate a stable passively Q-switched Raman fiber laser (RFL) operated in C- band region by incorporating Two-dimension (2D) material inside the ring cavity as saturable absorber (SA) such as titanium dioxide (TiO_2) and molybdenum disulfide (MoS_2). 2D materials have been experimented to generate pulse laser due to their unique electronic and optical properties such as modulation depth, saturable absorption and their recovery time. First, we conducted an experiment for Q-switched RFL incorporating MoS_2 based SA. The SA is prepared by depositing a mechanically exfoliated MoS_2 on the end of the fiber ferrule which is then connected to another clean ferrule via an optical fiber adapter. The cavity consist of dispersion compensating fiber (DCF) with a 7.7 km length and 584 $ps \cdot nm^{-1}$ km^{-1} of dispersion as nonlinear gain medium for Q-switching pulse train generation. The total laser cavity length is about 8 km. The Q-switching pulse train operated at around 1560.2 nm with the repetition rate changed from 132.7 to 137.4 kHz as the input pump power is tuned from 395 to 422 mW, while the pulse width reduced from 3.35 to 3.03 μs. At the maximum pump power of 422 mW, the maximum pulse energy of 54.3 nJ is achieved. Next, we conducted a Q-switched RFL by replacing the MoS_2 with TiO_2 film based SA. We observed that the pulse train operated at 1558.5 nm is generated with the repetition rate that can be increased from 131.4 to 142.5 kHz as the input pump power changed from 398 to 431 mW. We noticed that the Q-switched pulse produced maximum energy of 5.81 nJ and pulse width of 2.97 μs at input pump power of 427 mW and 431 mW, respectively. These results verified that the TiO_2 film and MoS_2 has a strong capability to be employed as an effective SA for Q-switched RFL pulse generation system.

Keywords: Q-switched, pulse, fiber laser

Q-SWITCHED RAMAN FIBER LASER BASED ON 2D MATERIALS AS SATURABLE ABSORBER

ABSTRAK

Tesis ini bertujuan untuk menunjukkan suis-Q pasif Raman serat laser (RFL) yang stabil yang beroperasi di julat jalur-C dengan menggabungkan material dua dimensi (2D) kedalam rongga membulat yang bertindak sebagai penyerap boleh-tepu (SA) seperti titanium dioksida (TiO_2) dan molibdenum disulfida (MoS_2). Material 2D telah didemonstrasikan untuk menghasilkan denyut laser disebabkan oleh sifat elektronik dan optik yang unik diantaranya penyerapan boleh-tepu, kedalaman modulasi dan masa pemulihan yang sangat pantas. Pertama, kami menjalankan kajian suis-Q RFL menggunakan filem MoS_2 sebagai SA. SA disediakan dengan mendepositkan pengelupasan mekanikal MoS_2 diatas permukaan ferul yang kemudiannya dipadankan dengan ferul lain yang bersih dengan menggunakan penyesuai optik. Jumlah panjang rongga dalam Raman serat laser ini kira-kira 8 km termasuk lah daripada serat penyebaran pampasan sepanjang 7.7 km (DCF) dengan 584 $ps \cdot nm^{-1}$ km^{-1} serakan digunakan sebagai medium pengganda tak linear untuk menjana denyut suis-Q. Hasilnya, denyut suis-Q beroperasi pada kira-kira 1560.2 nm dengan kadar pengulangan meningkat daripada 132.7 kHz kepada 137.4 kHz apabila kuasa pam ditala daripada 395 mW kepada 422 mW, manakala lebar denyut dikurangkan daripada 3.35 μs kepada 3.03 μs. Pada kuasa pam maksimum 422 mW, tenaga denyut tertinggi 54.3 nJ dicapai. Kemudian, kami meneruskan dengan menjalankan satu lagi kajian untuk menghasilkan suis-Q dengan menggantikan MoS_2 dengan TiO_2 filem berasaskan SA. Kami memerhatikan bahawa denyut yang beroperasi pada 1558.5 nm dihasilkan dengan kadar pengulangan yang boleh ditala daripada 131.4 kHz kepada 142.5 kHz apabila kuasa pam berubah daripada 398 mW kepada 431 mW. Adalah diperhatikan bahawa denyut suis-Q menghasilkan tenaga tertinggi dengan 5.81 nJ dan denyut lebar 2.97 μs pada

kuasa pam masing-masing 427 mW dan 431 mW. Keputusan ini mengesahkan bahawa TiO_2 filem dan MoS_2 mempunyai keupayaan besar untuk digunakan sebagai SA yang berkesan dalam menjana denyut pasif suis-Q Raman serat laser.

Kata kunci: Suis-Q, denyut, serat laser

ACKNOWLEDGEMENTS

Alhamdulillah, thanks to Allah for his blessing, opportunity and mercy along the journey to complete this thesis. I wish to express my gratitude to my supervisors Dr. Zamani bin Zulkifli and Prof. Dr. Harith Ahmad for giving me the opportunity to be one of their student and keep giving their help, supervision and advices from the early stage of this study.

I sincerely thank Prof. Dr. Sulaiman Wadi Harun, for his advice, help and ideas during the completion of this study and for guiding and reviewing me in the thesis writing. Also to PhD student Anas Abdul Latiff and En Faizal Ismail who presented consistent concern and helpful advice regarding my research. Without their continual guidance, this dissertation might not be able to complete. My gratitude also goes to my wonderful lab mate at Photonic Research Centre (PRC) especially Aisah, kak Umi, Ezza, Amelia, kak. Ahya and Fiqa for their help and motivation during progress of my research.

Last but not least, my greatest appreciation extends to my beloved family, especially to my parents Hisamuddin Suhaimee and Janah Tijo, also to my wonderful husband, Mohd Hazam bin Ishak and my adorable daughter, Raifa Qaisara for their fully understanding, prayers and endless love. I am really grateful to have all of you in my life. Alhamdulillah.

Thank you,

Najwa binti Hisamuddin

University of Malaya

2017

TABLE OF CONTENTS

LIST OF FIGURES

LIST OF TABLES

LIST OF SYMBOLS AND ABBREVIATIONS

A_{eff}	:	Effective area
c	:	Velocity of light.
E_c	:	Conduction band
E_v	:	Valence band
g_R	:	Coefficient of Raman gain
L_{eff}	:	Effective length
n	:	Refractive index (RI) of medium
P_0	:	Pump power at amplifier input
ASE	:	Amplified spontaneous emission
BP	:	Black phosphorus
CNT	:	Carbon nanotube
CW	:	Continuous wave
DCF	:	Dispersion compensating fiber
DCM	:	Dispersion compensating module
DSF	:	Dispersion shifted fiber
DRA	:	Distributed Raman amplifier
EDFA	:	Erbium-doped fiber amplifier
eDOS	:	Electron density of state
Er^{3+}	:	Erbium
FC/PC	:	Ferrule connector/physical contact
FESEM	:	Field-emission scanning electron microscopy
HRA	:	Hybrid Raman amplifier
ISO	:	Isolator
LD	:	Laser diode
LRA	:	Lumped Raman amplifier

MoS_2	:	Molybdenum disulfide
$MoSe_2$	:	Molybdenum diselenide
Nd^{3+}	:	Neodymium
NF	:	Noise figure
OC	:	Optical circulator
OSA	:	Optical spectrum analyser
OSC	:	Oscilloscope
OSNR	:	Optical signal to noise ratio
Pr^{3+}	:	Praseodymium
PVA	:	Polyvinyl alcohol
RA	:	Raman amplifier
RFL	:	Raman fiber laser
RFSA	:	Radio frequency spectrum analyser
RI	:	Refractive index
RP	:	Raman pump
SA	:	Saturable absorber
SESAM	:	Semiconductor saturable absorber mirror
SMF	:	Single mode fiber
SNR	:	Signal to noise ratio
SOA	:	Semiconductor optical amplifier
SRS	:	Stimulated Raman scattering
TiO_2	:	Titanium dioxide
Tm^{3+}	:	Thulium
TLS	:	Tunable laser sources
TMDCs	:	Transition metal dichalcogenides
TMO	:	Transition metal oxides

WDM	:	Wavelength division multiplexing
WS_2	:	Tungsten diselenide

CHAPTER 1: INTRODUCTION

1.1 Introduction

Recently, the demand for fiber lasers has grown tremendously. There is intense research on fiber laser in the high power region due to their criteria to overcome the limitation in solid-state lasers like compactness, flexibility and gain efficiency (Set & Yaguchi et al., 2004). Fiber laser is a type of laser that is made up from optical fiber doped with rare-earth element as active gain medium. For instant, erbium (Er^{3+}), thulium (Tm^{3+}), praseodymium (Pr^{3+}) and neodymium (Nd^{3+}). It offers several advantages such as low loss and great possibility of pumping with compact and efficient laser diode. The first demonstrations with gain fibers were conducted in the beginning of 1960 century (Snitzer, 1961; Koester et al., 1964). A flash lamp Nd^{3+} doped fiber with a 10 um of core diameter and 1 m length of fiber was utilized and were reported. Since then, it has been developed greatly and become practical especially in the optical communication. However, there are limitations of wavelength when utilizing the rare-earth doped fibers where it emits in fixed spectral bands and need diode laser emission spectrum to overlap with the absorption band.

Conversely, in Raman fiber lasers (RFLs) any Raman laser wavelength can be accessed in generating power and gain with optical fiber which the emission wavelength is depend on the Raman shift and the pump wavelength (Yao et al., 2015; Schröder et al., 2006), thus work as gain medium for a fiber laser.

A basic ring configuration for laser generation is shown in Figure 1.1 where the pump light is injected from the left-hand side through a wavelength division multiplexing (WDM), gain medium and optical circulator (OC). Generated laser light can be observed in Optical Spectrum analyzer (OSA).

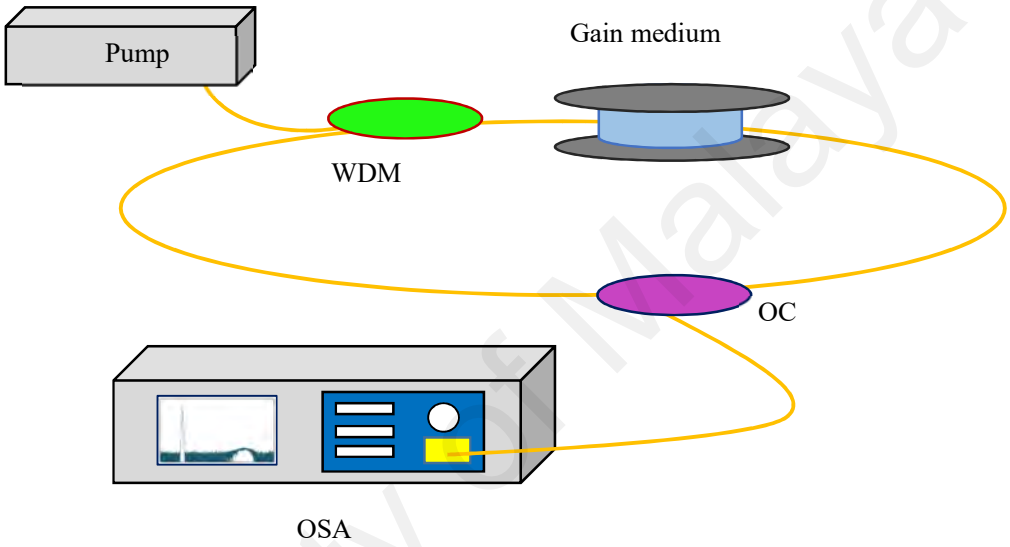

Figure 1.1: A ring configuration for basic fiber laser generation.

1.2 Fiber Laser Operation Modes and Their Applications

In general, laser sources can be classified into two modes of laser operations. First is continuous wave (CW) that generate light at constant output over time and is maintained by a pump source. Second, pulse operations which are mode locked and Q-switching (giant pulse formation) that produces light pulses at certain frequency as shown in Table 1.1.

Table 1.1: Summary of laser operation modes.

Operation mode	Definition	Typical pulse length
Continuous wave (CW)	Laser with constant frequency and amplitude	Less than 0.2 s
Q-switching	Deliver energy pulses in very short duration	1 μs – 1 ns
Mode locked	Emits a pulses train of extremely short duration.	Less than 1 ns

Continuous wave and pulse fiber laser offers several applications in various field such as in the telecommunication industries where those involving the data signal transmission over distances of less than a meter to hundreds of kilometers. It plays an important role in bio-medical industries which is applied in most modern telemedicine devices for transmission of digital diagnostic images (Clowes, 2008). Apart from that, it is also applied in the field of spectroscopy, laser material processing such as material cutting, metrology, scientific research, imaging and ranging (Knox, 2000; Set et al., 2004). Specifically, ultrafast mode locked and Q-switched fiber lasers pulse became more interest in the field of micro-machining (Fermann & Hartl, 2013; Martinez & Sun,

2013; Liu, X and Du et al., 1997), tissue welding (Kim et al., 2003), medical community such as dermatology, eye and dental surgeries (Juhasz et al., 1999; Chamorovskiy et al., 2012), optical sensor, temperature measurement and LIDAR (Henderson et al., 1993). Q-switching and mode locked can be achieved either using active or passive technique. The described laser operation modes can be achieved by incorporating the appropriate SA inside the fiber laser cavity that will be explained in details in the next chapter.

1.3 Problem Statement

The research interest towards Q-switched pulse fiber laser are increasing over the last decades due to their potential to generate shorter pulse durations and higher pulse energies which offers significant application in various field (Limpert et al., 2006). Recently, semiconductor saturable absorber mirrors (SESAMs) are utilized in available laser system due to their possibility to obtain desired parameter such as the saturation fluence and the modulation depth (Keller et al., 1996; Maas et al., 2008). Unfortunately, SESAMs have limited operation bandwidth. Moreover, SESAMs require a very costly and complex fabrication process (Sotor et al., 2015; Zhang et al., 2012; Popa et al., 2011). Therefore, there is a great development for new material for saturable absorber (SA) that able to operate in a wide range wavelength, easy and low fabrication cost.

1.4 Objectives of Thesis

The main objectives of this thesis are:

- To characterize Raman fiber laser.
- To propose and demonstrate passively Q-switching Raman fiber laser by employing different type of 2D materials as saturable absorber -Titanium dioxide (TiO_2) and Molybdenum disulfide (MoS_2).
- To analyze the performances of MoS_2 and TiO_2 as saturable absorber in Q-switched pulse generation.

1.5 Thesis Overview

This thesis is structured into six main chapters including the introduction and conclusion. First chapter outlines the basic introduction of fiber laser operation mode and their application, problem statement and main objective of the research. Chapter 2 focused on the theoretical background of passive Q-switched fiber laser technique. It leads higher pulse energy, having lower pulse repetition rates and offer longer pulse durations compared to mode locked. Working mechanism of saturable absorber (SA) and two dimension (2D) materials is also explained in details in this chapter. Besides, this chapter also describes about Raman amplifier (RA) and the differences between RA and erbium doped fiber amplifier (EDFA).

Chapter 3 investigates the Raman gain and noise figure in dispersion compensating fiber (DCF). This chapter also provides the experimental work on passive Q-switched Raman fiber laser based on MoS_2 as SA. The MoS_2 film was prepared by using mechanical exfoliation method that provides major advantages due to their reliability and its simplicity. In Chapter 4, Q-switched Raman fiber laser with TiO_2 film was demonstrated to figure out their performance as SA. Fabrication and characterization of TiO_2 film including the Raman spectrum is also highlighted in this

chapter. The experimental results and details explanation is described in Chapter 3 and 4. Chapter 5 concludes the performance of MoS_2 and TiO_2 film as SA and some recommendation that can be done for future work.

CHAPTER 2: THEORETICAL BACKGROUND

2.1 Introduction

Q-switching is an alternative technique to generate a pulse laser instead of mode locked. Q-switching leads to higher pulse energy, having lower pulse repetition rates and offer longer pulse durations compared to mode locked technique (Liu et al., 2013; Zhao et al., 2014; Harun et al.,2013). Even though Q-switching does not produce the shortest pulses like mode-locking, it has several advantages because it is easier to implement, efficient operation and low cost needed than the mode locked (Popa et al., 2011; Harun et al., 2012).

In Q-switched technique, conventional laser can be pulsed by modulating the losses inside the laser resonator. When the resonator losses are high (that is the Q factor is low), the population inversion builds up and suddenly released as the losses are saturated producing a powerful pulse which is sometimes called as 'giant pulse'. The Q-factor usually known as quality factor which can be described as:

$$Q = 2\pi v_0 \left(\frac{W}{\text{energy lost / second}}\right) \tag{2.1}$$

It can be simplified as below:

$$Q = 2\pi v_0 \left(\frac{W}{\delta Wc/n}\right) = \frac{2\pi nL}{\delta\lambda_0} \tag{2.2}$$

From the equation, correlation between the Q value and resonator loss (δ) which is inversely proportional when the value of λ_0 and L are definite. v_0 is defined as the frequency of the laser central. W is the energy stored in the cavity. The energy lost per second can be expressed by $\frac{\delta Wc}{nL}$, where δ is the energy loss rate for single-path of light that propagate in the laser cavity. L and n is the length of the resonator and refractive

index (RI) of medium, respectively. RI measures the speed of light in a vacuum to the speed of light in a matter $[c/v]$ and c is the velocity of light with the value of 3.0 x 10^8 m/s.

Q-switched fiber lasers have a huge range of application such as in the telecommunication, remote sensing, material processing, military and fiber sensing. It has also become significant in the medical community and is applied in the medical laser surgery for removing tattoo, pigmented lesions and hair removal (Bai et al., 1882; Tiu et al., 2014; Kurkov, 2011). This is due to the high pulse energy and short pulse width that can be constructed via active or passive techniques. Basically, active Q-switching can be achieved by placing external modulation such as acousto optic effect and rotating mirror. Passive Q-switching technique used a saturable absorber inside the laser cavity and this technique has more advantages such as cost effectiveness (by removing the electronic and its modulator), compactness and simplicity of design as compared to active Q-switched technique (Dong et al., 2010; Saidin et al., 2013). As well as mode locked, it can be generated either in active or passive. Active mode locked depends on an external source placed in the laser cavity. Meanwhile, passive mode locked technique do not require an external source to generate pulse, rather they use the cavity light itself to incite a change within laser cavity. The difference between Q-switching and mode locked lies in the optical phase of the pulses where mode locked pulses are phase coherent with each other. Meanwhile the Q-switched pulses are not (Hudson, 2009). In this research work, we are focused on the passively Q-switched fiber laser using Raman pump power and 2D (two dimensional) materials will be utilized as an SA in order to generate the laser that operates in nanosecond or microsecond region.

2.2 Passively Q-switched Fiber Laser

Passive Q-switched fiber laser is generated when the cavity losses are modulated with saturable absorber (SA). As the gain has achieved an adequate high level, the pulse laser is clearly formed. SA becomes a key element for pulse laser generation. By placing SA instead of modulator and its electronics, making this method simpler and cost effective as compared to active Q-switched (Luo et al., 1999; Saidin et al., 2013). SA is an optical component that initially introduces a certain optical loss. It happen when the absorbing materials is excite to an excited state and decreasing the population in the ground state. SA is a material that reduces the absorption of light with the rising of the intensity of light. As the level of intensity is high enough, the saturated material produce a high transmission output. There is a significant parameter to determine the ability of SA, such as ultrafast recovery time (around picosecond), broadband absorption, high damage threshold, modulation depth and the fabrication cost (Schibli et al., 2005). SA recovery time is much longer than the ideal pulse duration, thus preventing the unnecessary energy loss. Nevertheless, the absorber should be quick enough to avoid the premature lasing when the gain recovers. Normally, recovery time is between upper-state lifetime of the gain medium is ideal and pulse duration. Basically, the SA only absorbs a minor portion of the energy of the generated pulse.

In principle, SA is a material that absorbs light depending on the intensity of the incident light, whether high or low intensity. A simple explanation of the phenomenon can be understood as eDOS (electron density of state) occupation in conduction bands of SA materials which consists of two energy levels: energy level of valence band (*Ev*) and energy level of conduction band (*Ec*). If the intensity of the incident light is low, photons are highly absorbed by the electron in the *Ev* to be excited up to *Ec*. Meanwhile, if the optical intensity of light is high, the absorbance of the photons decreases due to the eDOS in *Ec* is occupied with other electron which excited by the

light (Kashiwagi et al., 2010). So that, by incorporating the SA inside cavity, light will pass through the SA which consists of low and high intensity that created high and low loss respectively. This situation propagate to high intensity contrast (Muhammad, 2014). Thus, light starts to oscillate in pulsed state. The working principle of the SA is depicted in a schematic diagram as shown in Figure 2.1.

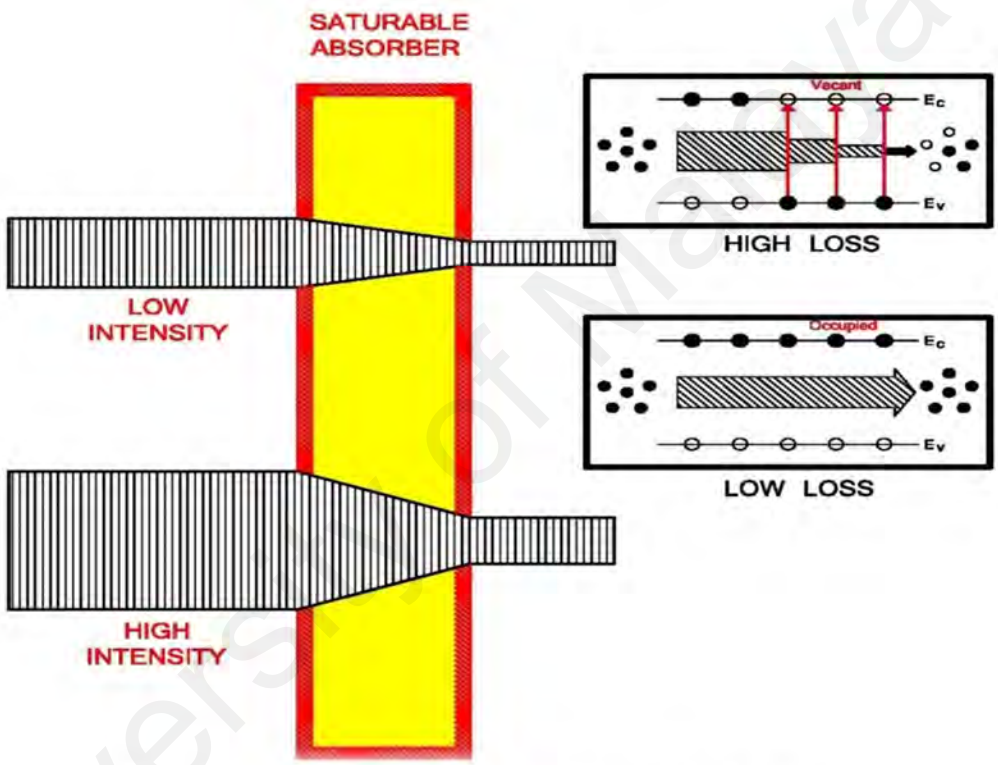

Figure 2.1: Working mechanism of saturable absorber.

2.3 Two Dimension (2D) Material

Nowadays, there is intense research on the SA due to the development of ultrafast fiber lasers applications. Recently, most of the available ultrafast laser systems generally use semiconductor saturable absorber mirrors (SESAMs) because of their outstanding performance to achieve desired optical criteria such as nano-saturable absorption, modulation depth, saturation fluence and recovery time (Martinez & Sun, 2013; Haiml et al., 2004). However, there is some limitations of SESAMs where their

operation bandwidth is relatively narrow and the absorbers have to be fabricated by very costly and complicated processes (Sotor et al., 2015; Liu et al., 2012). These factor has attracted a great attention in the development of new SA based on carbon nano-materials such as carbon nanotubes and graphene (Jiang et al., 2015). The effective applications of graphene has encourage the exploration of 2D materials in which the layer structure results in weak inter-layer van der Waals coupling and strong intra-layer covalent bonding (Zhang et al., 2014). In particular, 2D materials could results strong optical saturable absorption due to their unique electronic and optical properties (Luo et al., 2016). In recent years, many 2D materials are discovered, for instance transition metal dichalcogenides (TMDCs) commonly molybdenum disulphide (MoS_2), molybdenum diselenide ($MoSe_2$) and tungsten diselenide (WS_2) (Wang et al., 2015; Chen et al., 2015), topological insulators such as Bi_2Se_3, Bi_2Te_3, and Sb_2Te_3 (Luo et al., 2013; Tang et al., 2013), transition metal oxides (TMO) for instance titanium dioxide (TiO_2) (Ahmad et al., 2016) and also black phosphorus (BP) (Luo et al., 2015; Li et al., 2015; Qin et al., 2015). The 2D materials give some opportunities for the cost effectiveness of fabrication process and flexible broadband saturable absorbers. 2D TMDs received massive attention due to their property in semiconducting with tunable bandgaps and abundance in nature (Wu et al., 2015). In these studies, we are going to demonstrate an experiment for passively Q-switched fiber laser generation by utilizing 2D materials which are TiO_2 and MoS_2 as SA.

2.4 Raman Amplifier

In the early of 1970s, Stolen and Ippen demonstrated the Raman amplification in optical fibers. However, Raman amplifiers (RA) remained primarily laboratory interest in the first half of the 1980s (Bromage, 2004). By the beginning of 2000s, RA are being utilized in almost all long haul systems (which is defined at transmission distance

around 300 km to 800 km) replacing the conventional amplifier which is widely used previously, erbium-doped fiber amplifiers (EDFA). This is due to the great demand in terms of transmission capacity that has been dramatically increased, thus fulfilling the whole spectral band of the EDFA which then required RA technology for wideband optical network (André et al., 2012).

There are several advantages in RA. First, due to the ability to tune the wavelength over a broad spectrum by deploying a different wavelength of Raman pump (RP). Normally, the preferred pump wavelength is 100 nm shorter than the gain spectrum needed (Krause et al., 2003; Ravet et al., 2004; Kuang et al., 2015). Second, Raman gain is present in any types of fiber that offers cost effectiveness. The third advantage, it is a relatively broad-band amplifier with a 5 THz bandwidth, and the gain is flat over a broad wavelength range. Apart from that, RA provide wider band and produce less gain than EDFA. However, there are some drawbacks of RA compared to the EDFAs since it has poor pumping efficiency at lower signal powers. But, this lack of pump efficiency makes gain clamping easier in RA. Other than that, longer gain fiber is required for RA. But, this weakness can be solved by adding dispersion compensation and the gain in a single fiber.

The signal in RA is enhances by Raman amplification, different from SOA and EDFA the amplification is created by the nonlinear interaction between the signal and pump laser inside an optical fiber as illustrated in the schematic diagram in Figure 2.2.

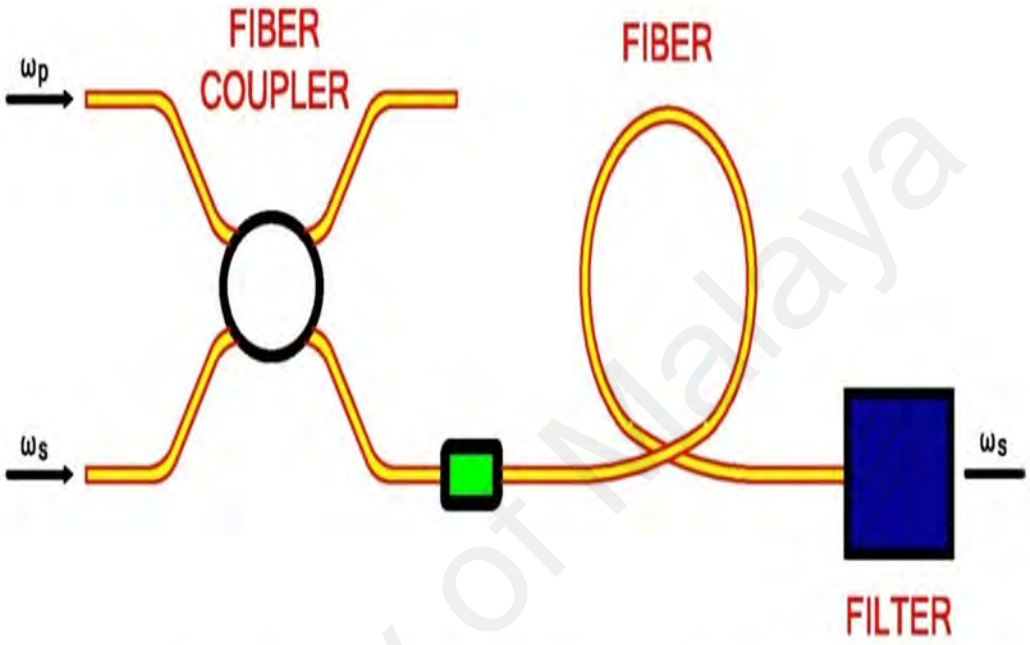

Figure 2.2: Schematic of a fiber Raman amplifier.

In ultrafast fiber laser application, Raman pump power has attracted a lot of interest due to the fact that it is an alternative way to generate the passive Q-switched instead of using laser diode (LD) as pump power. For this study, we are using a RP acts as a pump sources for the nonlinear gain mechanism. RP required high pump power and longer fiber to generate high nonlinear effect.

Figure 2.3 shows the spectrum of Raman gain for single mode fiber (SMF) with the highest gain achieved at 13.2 THz and the Raman gain bandwidth is around 40 THz wide at the pump wavelength of 1550 nm. In telecommunication bands, it corresponds to about 100 nm. The gain bandwidth within the wavelength position can be simply tuned by changing the wavelength of the pump.

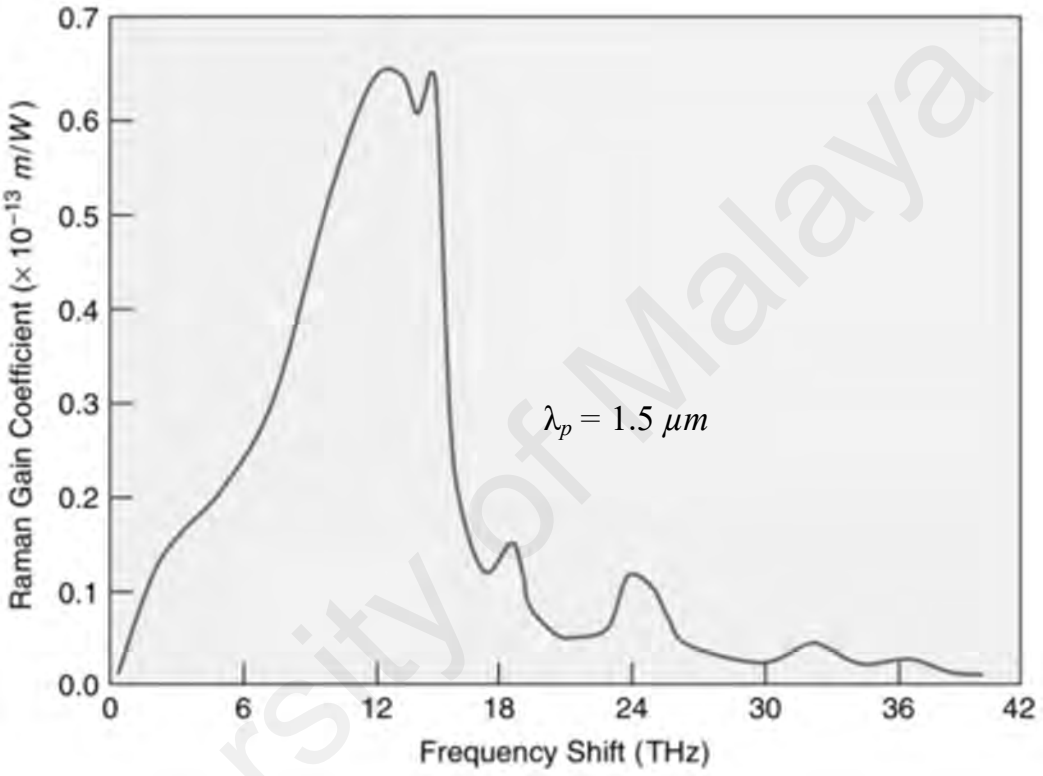

Figure 2.3: Raman gain coefficient graph.

In RA, the gain amplifier G is defined by:

$$G = \exp\ (g_R P_0 L_{eff} /\ A_{eff}) \quad (2.3)$$

Where,

g_R is the coefficient of Raman gain. In fiber, g_R is depends on the fiber core composition and varies with different type of dopant. P_0 is the pump power at amplifier input and L_{eff} is effective length. A_{eff} is the effective core area of fiber. Different fiber has different value of A_{eff}. Based on the equation 2.3 to increase the efficiency of Raman gain, we need higher coefficient of Raman gain g_R and smaller effective core

area, A_{eff}. In this study, DCF with smallest effective area around 15 μm^2 will be used as gain medium.

2.4.1 Types of Raman Amplifier

Basically, Raman Amplifier (RA) amplification can be obtained by the interaction of Raman pump (RP), high nonlinear effect of fiber and signal. It can be classified into three categories as shown in Figure 2.4. The first one is distributed Raman amplifier (DRA), which the transmission fiber itself is employed as the gain media by multiplexing a signal wavelength and pump wavelength, with a backward pump injected over the fiber (typical fiber length is more than 40 km). Second is discrete Raman amplifier or also known as lumped Raman amplifier (LRA) where a dedicated length of fiber is inserted into the transmission line to create amplification (typical fiber length is about 5 km). LRA requires highly nonlinear fiber with a small effective area of fiber core to enhance the interaction between the pump wavelengths and signal, thus reducing the fiber length. Conclude that LRA requires a shorter length of fiber to provide amplification. The third category is hybrid Raman amplifier (HRA) where it combines two gain media together.

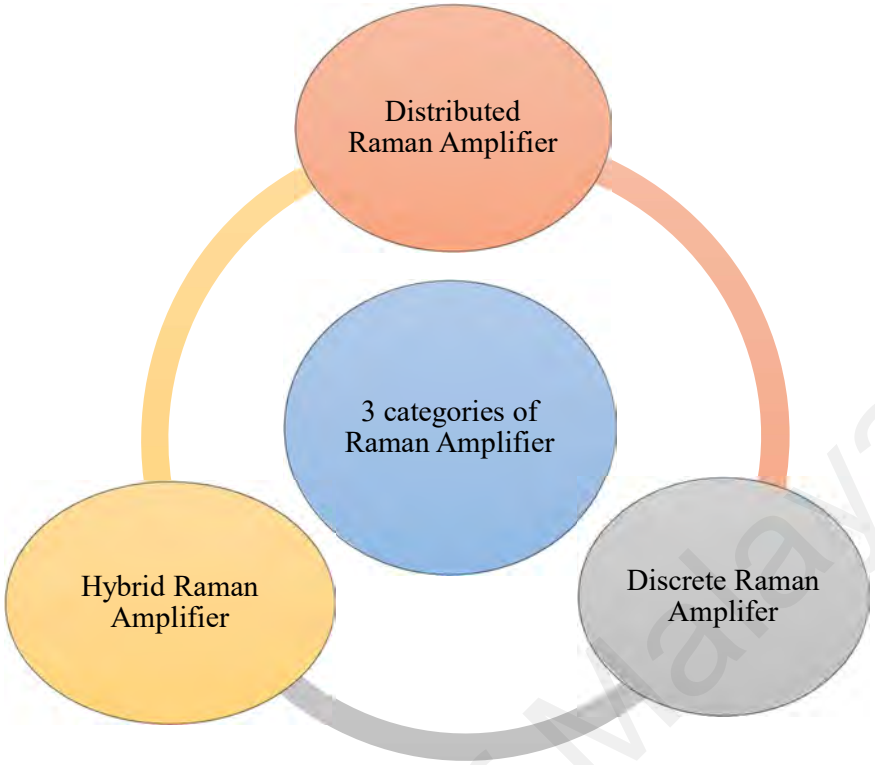

Figure 2.4: Categories of Raman amplifier.

2.4.2 Spontaneous and Stimulated Raman Scattering

In 1982, Raman scattering was discovered by a physicist from India, Sir Chandasekhar Venkata Raman that earned him the Nobel Prize in 1930. Raman scattering explains a process where the light photons are scattered from a shorter wavelength to a longer wavelength (lower energy) (Headley & Agrawal, 2005). Raman scattering can be classified into two categories, which are stimulated and spontaneous Raman scattering. In 1928, spontaneous Raman scattering, was observed by Landsberg, Mandelstam and Raman.

It happen when an incident light is scattered from the molecules of a substance, with the scattered light consist most of the light with same frequency and energy as the incident light. At the same time, low intensity light with lower and higher energy than the incident light can be observed. The working principle behind Raman amplifier is

called stimulated Raman scattering (SRS). SRS is a nonlinear effect of optical fiber which has advantages of self-phase matching between the pump and signal and also created wide bandwidth or high speed response as compared with other nonlinear processes (Kang et al., 2002). Over the last decade the interest in the SRS has increased significantly with the development of optical telecommunication. SRS is a very significant non-linear effect because it affects wavelength division multiplexing (WDM) and signal to noise ratio (SNR).

Figure 2.5 describes that the photon of the pump (ω pump) is excited to virtual state and then scattered by molecule in the fiber medium which is then relaxes to the lower state and become the lower energy photon (ω stokes) by emitting photon as well as vibrational energy, naturally the emitted photon has less energy than incident photon, and therefore a longer wavelength (thus provide amplification).The difference between the frequency of ω pump and ω stokes has to match a relationship in order to fully use of this nonlinear effect.

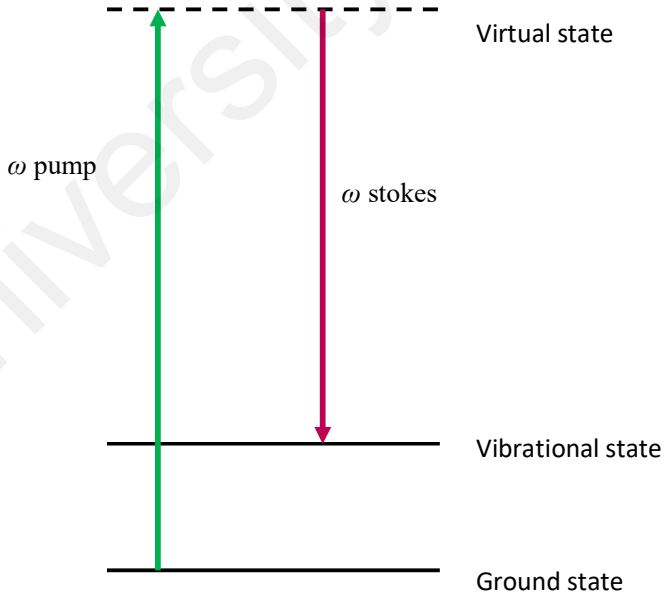

Figure 2.5: Stimulated Raman scattering (SRS) energy diagram.

2.5 Comparison of Raman Amplifier and EDFA

The gain spectrum of erbium doped fiber amplifier (EDFA) is determined by the erbium atoms. Unlike Raman amplifier (RA), where the gain spectrum is depends on the pump wavelength. The main drawback for RA requires higher pump power compared to the pump power in EDFA. Other differences between both amplifier are shown in Table 2.1 (Namiki & Emori, 2001).

Table 2.1: Comparison between RA and EDFA.

Characteristic	RA	EDFA
Amplification band	Depends on avaibility pump wavelength	Depends on dopant
Pumping wavelength	100 nm lower than signal required	980 nm or 1480 nm for EDFAs
Bandwidth	Good for C, L and S band	Good for C band and not bad for L band
Gain	Proportional to pump intensity and fiber length	Depends on ion concentration, fiber length and pump configuration
Saturation power	Equals about power of pump waves	Depends on doping, pump direction, gain cross section and exited state lifetime
Noise	Higher	Lower

2.6 Parameters for Dispersion Compensation Fiber

Raman amplifier (RA) can be achieved with different kind of fibers which provide a cost effective (Islam, 2003). However, high pump power and long interaction length of fiber are required in order to produce high nonlinear effect. High nonlinearity is significant to generate required Raman gain. For this study, a 7.7 km long of dispersion compensating fiber (DCF) is used as gain medium since it has good element for Raman amplification such as high nonlinearity and small effective area compared to others fiber. The specification of dispersion compensation fiber (DCF) used is listed in the Table 2.2.

Table 2.2: The parameters for 7.7 km DCF.

Parameters	DCF
Length of fiber (km)	7.7
Effective mode area (μm^2)	15
Dispersion (ps/nm*km)	-584
Attenuation loss at 1530 nm ($dBkm^{-1}$)	1.5
Attenuation loss at 1550 nm ($dBkm^{-1}$)	0.65

Table 2.3 and Figure 2.6 shows the comparison of effective area at wavelength of 1550 nm for different type of fiber and the Raman gain profiles at 1510 nm pump for different types of fiber, respectively. It compares a few types of fiber including single mode fiber (SMF), non-zero dispersion-shifted fiber (NZDSF), dispersion shifted fiber (DSF) and dispersion compensating fiber (DSF). From these table and figure, we can easily compare and conclude that the DCF is a highly suitable candidate for Raman gain medium due to its high Raman gain efficiency and it has the smallest effective area at around 15 μm^2 that tend to create better nonlinear effect (Rasmus, 2008) (Mohd Zamani, 2012).

Table 2.3: The effective area of different fiber types.

Type of fiber	**Effective Area at 1550 nm (μm^2)**
SMF	72-80
NZDSF	55-72
DSF	45-50
DCF	15

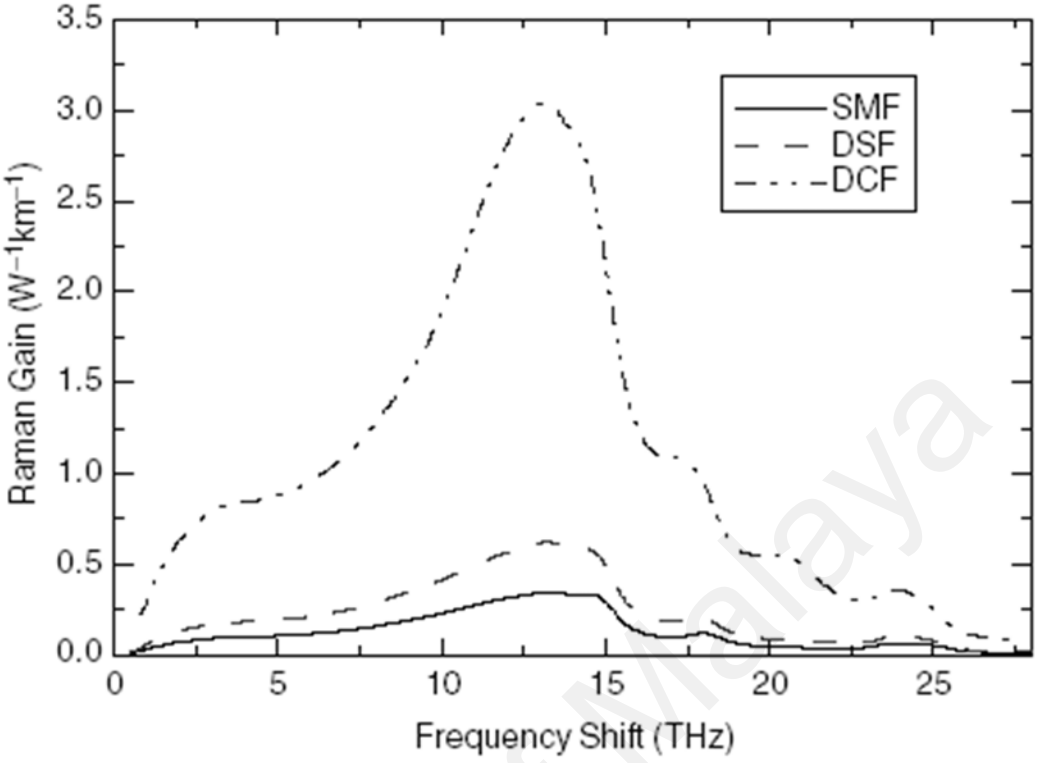

Figure 2.6: Profiles of Raman gain at 1510 nm pump in three different fiber types.

CHAPTER 3: PASSIVELY Q-SWITCHED RAMAN FIBER LASER INCORPORATING MoS_2 AS SATURABLE ABSORBER

3.1 Introduction

Recently, graphene has been studied extensively as a saturable absorber (SA) for short optical pulse generation due to their large absorption of incident light and optical nonlinear properties (Bonaccorso et al., 2011; Nair et al., 2008; Bonaccorso et al., 2010), but there is some limitation where the operation bandwidth of graphene SA is limited by the bandwidth of substrate (Ma et al., 2014). Most recently, there is a growing interest in 2D TMDs material which has high third-order nonlinear susceptibility (Wang et al., 2014), exhibit saturable absorption (Woodward et al., 2015) (Khazaeinezhad et al., 2015) and offers high damage threshold. For instance Molybdenum disulfide (MoS_2) is reported to have stronger nonlinear optical respond, better saturable absorption and lower saturation intensity as compared to graphene (Ahmad et al., 2016). The MoS_2 has future application at visible wavelengths based on their direct bandgap of 1.9 eV (Kuc et al., 2011). Characterization of saturable absorption in MoS_2 by Wang (Nanosheets et al., 2013) begins an advance wave of research on 2D materials for short pulse generation. In recent, the measurement of saturable absorption of MoS_2 was also conducted at 800 nm by using the Z-scan approach (Zhang et al., 2014). As far as we know, Q-switched RFL pulses propagate in any wavelength regime utilizing a passive SA has never been conducted before. The earlier research focused on graphene nanomaterials and carbonannotubes (CNT) employing a doped fiber as a gain media (Jun et al., 2015; Harun et al., 2012; Bao et al., 2014). Previously, most of the research studies about RFL focused on continuous wave (CW) operation (Rong et al., 2003; Pei et al., 2006). In this study, we demonstrate an experiment for passively Q-switched RFL employing a MoS_2 as SA and a 7.7 km

long dispersion compensating fiber (DCF) as nonlinear gain medium. From our observation, at a maximum pump power of 422 mW, the repetition rate can be tuned from 132.7 to 137.4 kHz with the highest pulse energy of 54.3 nJ and the shortest pulsewidth of 3.03 μs.

3.2 Investigation of Raman Gain and Noise Figure in Dispersion Compensating Fiber (DCF)

Fiber optic communication has become applicable for more than 30 years and there has been a progressing stream of technological development. The growing interest towards internet has led to the introduction of DWDM systems. With the tremendous increase in demand for communications capacity in past few years, interest has been focused on RA, and work goes ahead on utilizing them for several systems. On the other hand, single-mode DCF are the most extensively utilize technology for dispersion compensation. DCF is an ideal Raman gain medium, where the efficiency gain is seven to ten times higher than standard single-mode fiber (SMF) (Nicholson, 2003). In this section, the Raman gain in a dispersion compensating module (DCM) based on 7.7 km DCF is investigated.

At first, the amplified spontaneous emission (ASE) of the nonlinear gain media is investigated by pumping with 1445 nm Raman pump laser. ASE is the dominant noise in an optical amplifier that is produced by spontaneous emission when the laser gain medium is pumped. When the lasing threshold is achieved, ASE feedback by the laser's optical cavity may create laser operation. Laser threshold can be described as the minimum level of excitation where output laser is dominated by stimulated emission instead of spontaneous emission.

In the experiment, 1445 nm Raman pump is launched into the DCF through a wavelength division multiplexer (WDM) as shown in Figure 3.1. The DCF is 7.7 km long with loss characteristic of about 0.4 dB for pumping and the amplification band.

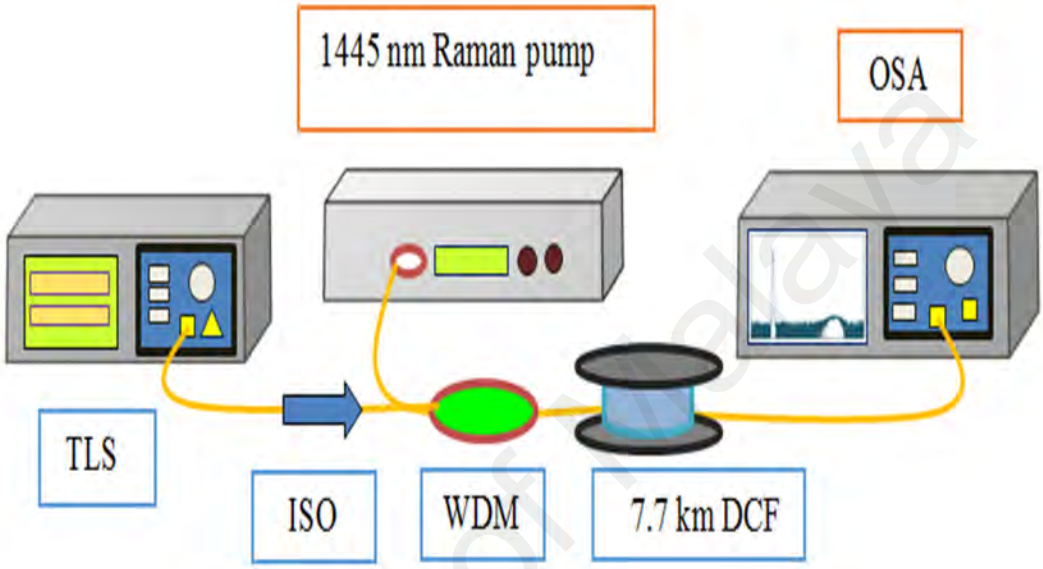

Figure 3.1: Experimental setup for measuring ASE spectrum and Raman gain.

Figure 3.2 depicted the experimental setup for characterization of 1455/1550 nm WDM. The 1455/1550 nm WDM was connected to the output of 1455 nm Raman pump (RP) and the output of WDM can be observed on optical power meter (OPM). Figure 3.3 shows the RP characterization measured before and after WDM by using an OPM. It is observed that by increasing the value of input power for every 20 mA, the output power before the WDM steadily increases from 50.9 to 1780 mW. After the WDM, the output power is reduced about 60 % where only 700 mW of the pump power is obtained at the maximum injected current of 9900 mA.

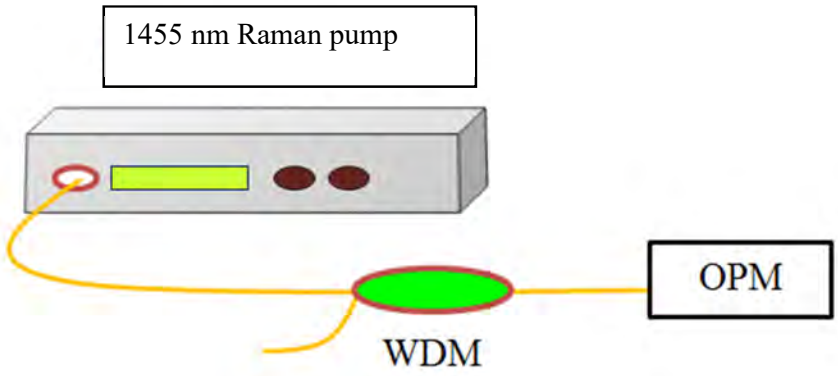

Figure 3.2: Experimental setup for characterization of 1455/1550 nm WDM.

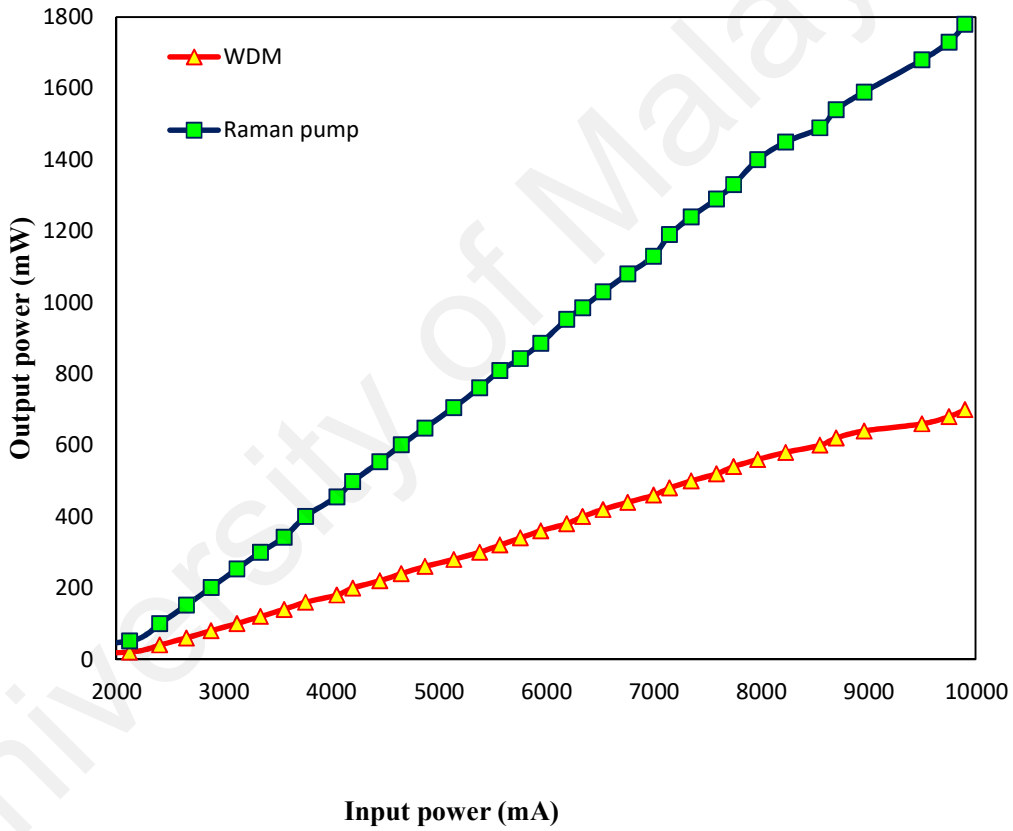

Figure 3.3: Output power against the input current for the Raman pump as measured before and after the WDM.

Figure 3.4 shows the output ASE spectrum as measured after the DCF by the OSA. Experiment is conducted with the pump power (after WDM) is fixed at 460 mW. It shows a residual pump at 1445 nm and ASE region centered at 1555 nm. The Raman ASE bandwidth covers from 1520 to 1570 nm. As shown in Figure 3.4, the highest ASE

power is obtained at around -63 dBm at 1555 nm. In Raman amplification, there are significant aspects that should be considered: 1) the pumping band loss since it is related to the Raman amplification efficiency, and 2) the coefficient of Rayleigh scattering has to be minimum as possible because it could leads problem like double Rayleigh back-scattering noise (multipath interference noise, or MPI). The ON/OFF gain of the DCF (7.7 km) was then measured by injecting an input signal from tunable laser source (TLS) into the Raman amplifier system as shown in Figure 3.1.

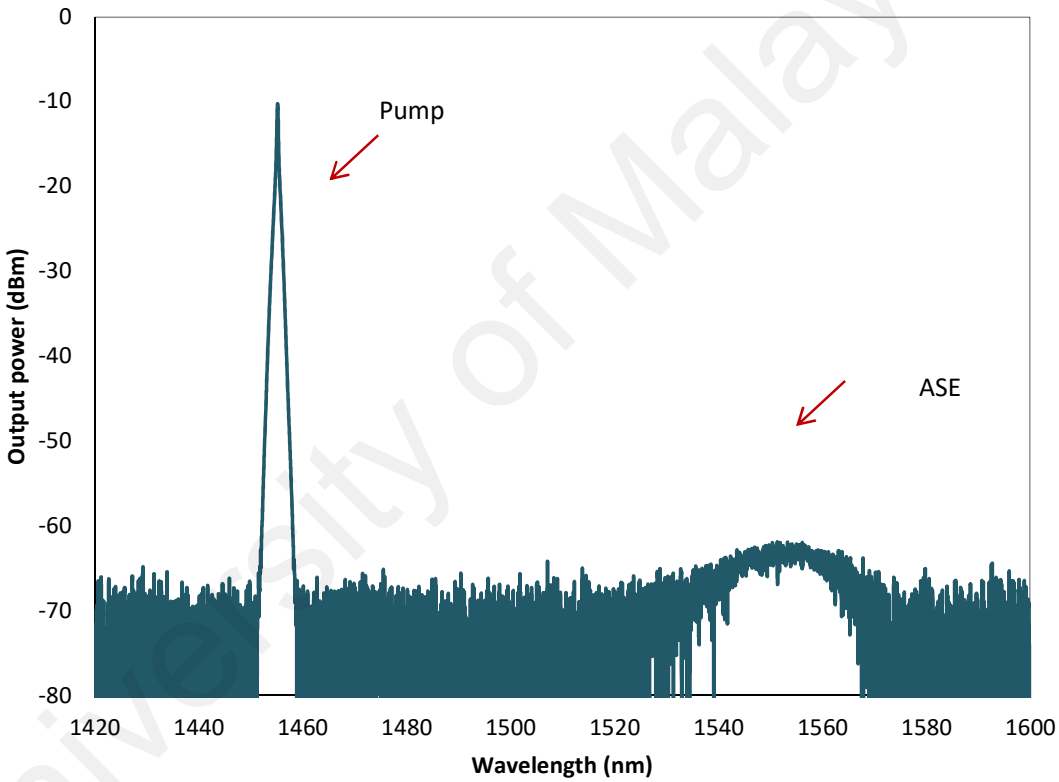

Figure 3.4: Raman ASE with 1445 nm pump power of 460 mW.

Figures 3.5(a), (b) and (c) show the ON/OFF gain of the Raman amplifier at input signal wavelengths of 1545 nm, 1555 nm and 1565 nm, respectively. The ON/OFF gain is measured by comparing the output signal with Raman pump ON and OFF condition. Raman pump (1445 nm) is fixed at 520 mW (or 1290 mW before WDM) while the input TLS power is fixed at -10 dBm. As shown in Figure 3.4, the

output signal power is increased as the Raman pump is on. This is attributed to the stimulated Raman scattering process, which transfer the energy from the Raman pump to the output signal through a nonlinear process. The ON/OFF gain of the Raman amplifier is summarized in Table 3.1. The gain varies from 12.04 dB to 12.44 dB within the signal wavelength of 1545 nm to 1565 nm. The maximum gain of 12.44 dB is obtained at input signal of 1545 nm. As the Raman pump power increases, the ON/OFF gain can be further increased.

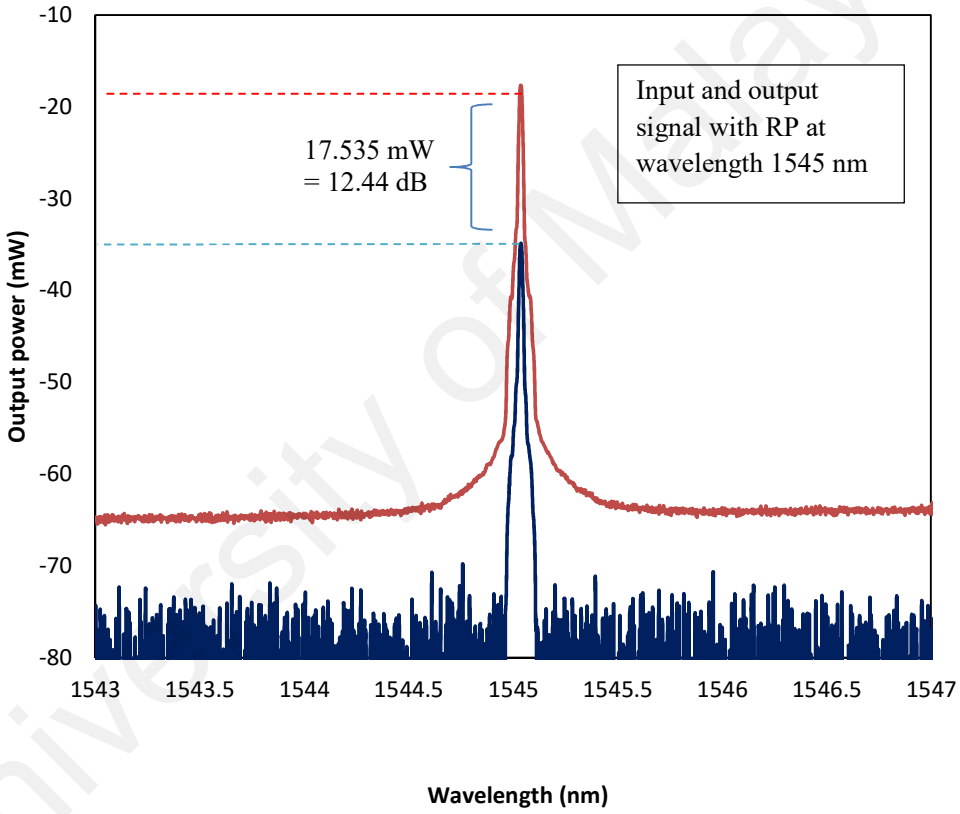

Figure 3.5(a): Input and output signal with Raman pump ON (red line) and OFF (blue line) at 1545 nm.

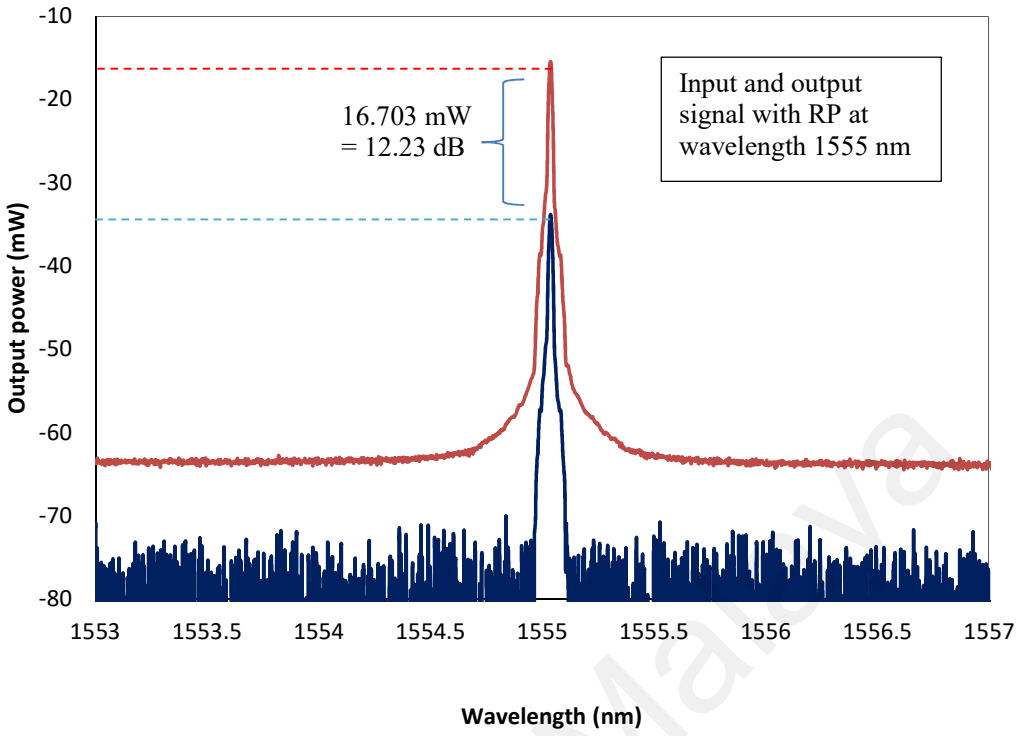

Figure 3.5(b): Input and output signal with Raman pump ON (red line) and OFF (blue line) at 1555 nm.

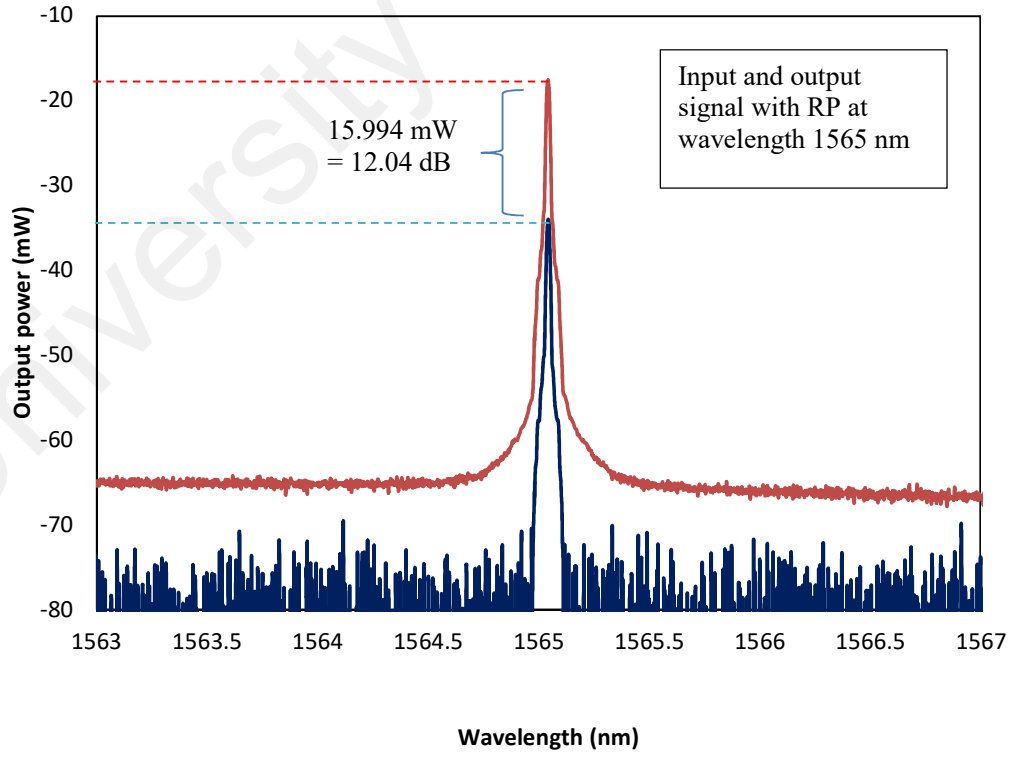

Figure 3.5(c): Input and output signal with Raman pump ON (red line) and OFF (blue line) at 1565 nm.

Table 3.1: ON-OFF Gain at three different wavelengths.

TLS wavelength (nm)	ON-OFF Gain
1545	12.44 dB
1555	12.23 dB
1565	12.04 dB

The noise figure of the RA is related to the optical signal to noise ratio (OSNR) of the output amplified signal. OSNR is described as the signal peak power over the noise of peak power within the system bandwidth. It can be expressed as the following equation;

$$OSNR\ (dB) = 10log_{10}\ \frac{Psignal\ (W)}{Pnoise\ (W)} = Psignal\ (dBm) - Pnoise(dBm) \quad (3.1)$$

The noise figure (*NF*) is a measure of the reduction of the SNR when the noise of amplifier adds to the signal. It can be defined by equation below:

$$Noise\ Figure\ (NF) = 10log_{10}(F) = SNR_{In} - SNR_{Out} \quad (3.2)$$

Where *F* is a noise factor for a system and is given as;

$$Noise\ Factor\ (F) = \frac{signal\ to\ noise\ ratio\ (in)}{signal\ to\ \ noise\ ratio\ (out)} \quad (3.3)$$

Based on Equation 3.2 and Figure 3.5, the *NF* of the RA is calculated for three different wavelengths and the results are simplified in Table 3.2. The NF of the RA is estimated to be around 8 dB.

Table 3.2: Noise figure at three different wavelengths.

TLS wavelength (nm)	Noise Figure
1545	7.76
1555	7.73
1565	8.17

In a closed cavity such as ring resonator, the ASE oscillates in the cavity to create laser based on the signal amplification by the Raman gain.

3.3 Sample Preparation of Molybdenum Disulfide (MoS_2)

The molybdenum disulfide (MoS_2) film was prepared by using mechanical exfoliation method (Hisamuddin et al., 2016). It has been extensively utilized in graphene based ultrafast fiber laser applications (Saleh et al., 2014; Martinez et al., 2011). The major advantages of mechanical exfoliation are due to their reliability and its simplicity, where the whole fabrication process does not require complicated procedures and expensive equipment. Thin flakes were peeled off from a big block of MoS_2 crystal by using scotch tape. The stuck flakes were repeatedly pressed to ensure it become thin enough in order to propagate light with high efficiency. Next, the thin flakes were transferred onto fiber ferrule end face before it is connected with another clean fiber

ferrule by using an optical fiber adapter. The Renishaw's Raman analyzer with a laser power of 5 mW and excitation wavelength of 532 nm was utilized to measure the Raman spectrum of the exfoliated MoS_2. This is one of the non-destructive methods that is extensively explored for vibration mode characterization and therefore the structure of nanomaterial. The generated Raman spectrum is shown in Figure 3.6(a), which indicated two bands of Raman characteristic at 378 cm^{-1} and 404 cm^{-1} (Yim et al., 2014;(Tongay et al., 2012), referring to the E^1_{2g} and A_{1g} modes of MoS_2, respectively. The number of MoS_2 layers can be determined by the difference of frequency peak between the vibration modes of in-plane (E^1_{2g}) and out-of-plane (A_{1g}). The difference of frequency for MoS_2 sample was about 25 cm^{-1}, which corresponds to a layer number of 2∼5 (Li et al., 2012). Figure 3.6(b) shows the field-emission scanning electron microscopy (FESEM) image of the exfoliated MoS_2, that defined the flakes size is about 2 x 5 μm. Nonlinear optical properties is a significant parameter in order to indicate the capability of every material to be recognized as an SA. The nonlinear transmission profile was recorded by injecting the C-band mode-locked laser source throughout a sample of SA's in twin-detector measurement configuration is depicted in Figure 3.6(c) with the power intensity against the transmission according to a simple two-level SA model (Garmire, 2000). The MoS_2 saturation intensity (I_{sat}) is 21.5 MW/cm^2 with modulation depth (α_s) of 11.8 %, and the non-saturable absorption (α_{ns}) is 27.7 % which confirms MoS_2 has adequate capacity as SA.

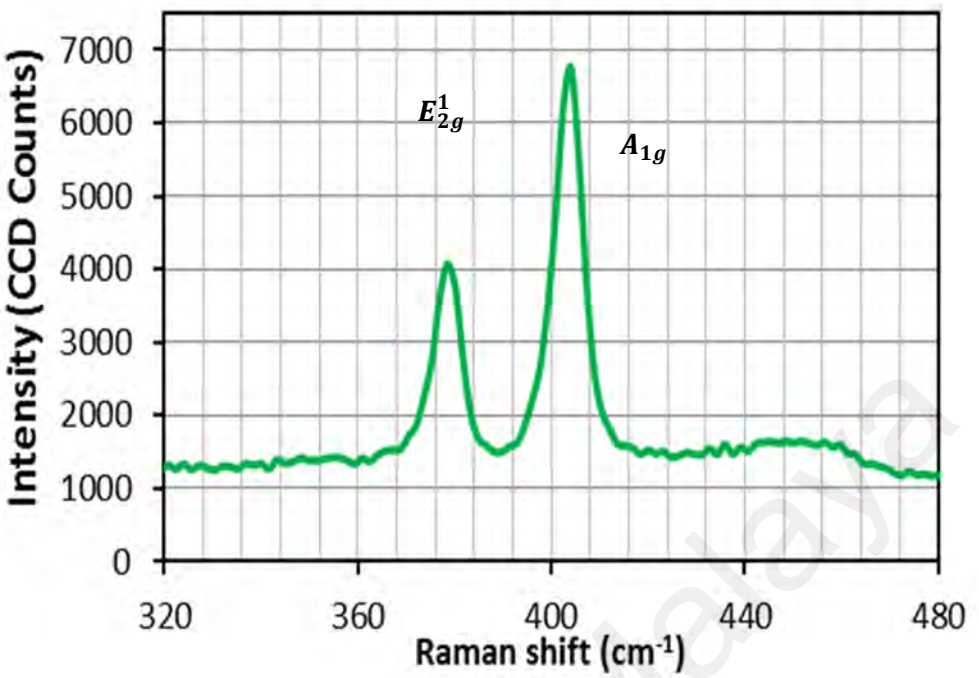

Figure 3.6(a): Raman spectrum.

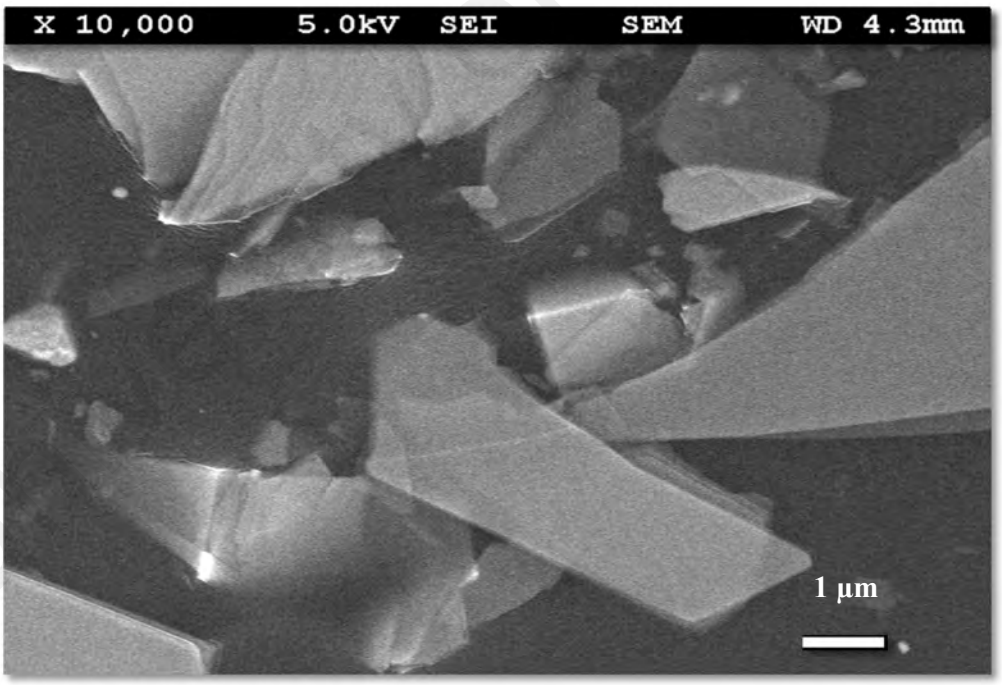

Figure 3.6(b): FESEM image.

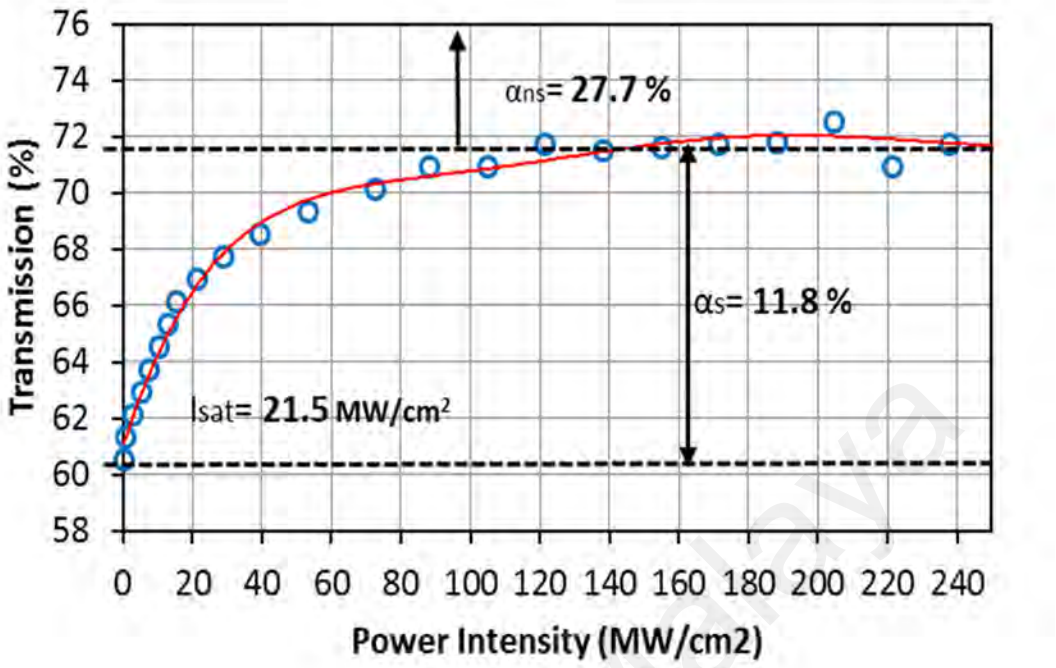

Figure 3.6(c): Nonlinear transmission profile.

The ring cavity of the proposed Q-switched Raman fiber laser is formed by incorporating MoS_2 as SA is shown in Figure 3.7. The system composes a DCF approximately 7.7 km in length, a 1455 nm Raman pump, a WDM, an optical isolator (ISO) and 95/5 fiber coupler. The signal is forward pumped through a WDM to combine the 1455 nm pump with a laser signal and the DCF with 584 ps/nm*km of dispersion (DCM LEAF 580) acts as a nonlinear gain media to produce amplification at the 1550 nm region. An ISO is placed after the DCF to assure that the light will propagate in one direction and suppress the Brillouin backscattering that induce pulse instability.

The experiment is conducted by depositing 1 mm x 1 mm area of MoS_2 film on the end face of the fiber connector and adheres with index matching gel serve as a SA for ultrashort pulse generation. A FC/FC optical adapter is used to connect the fiber connector with the deposited MoS_2 with a 95/5 fiber coupler. The 5 % output port was

used to measure the spectrum and the pulses train by using an optical spectrum analyzer (OSA) with 0.02 nm wavelength of resolution and a 350 MHz digital oscilloscope (OSC), 1.2 GHz photodetector together with 7.8 GHz radio frequency spectrum analyser (RFSA), respectively.

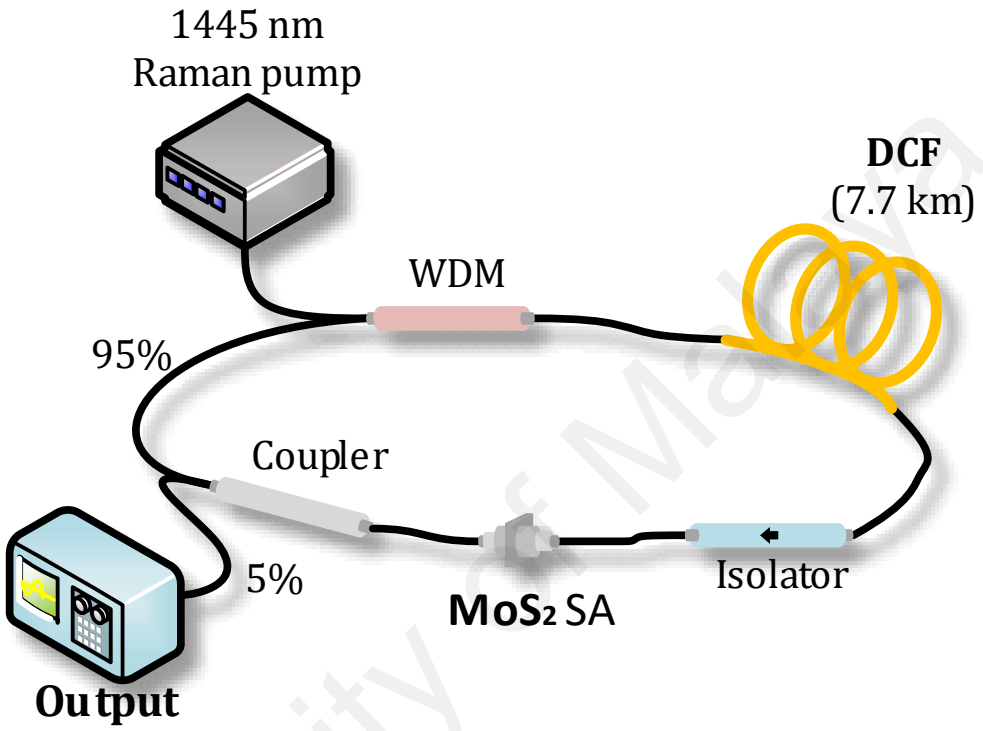

Figure 3.7: Schematic diagram of the proposed Q-switched RFL with a ring cavity.

3.4 Performance of the Q-switched Raman Fiber Laser with MoS_2

Figure 3.8 shows the optical spectra of the Q-switched pulse RFL at 422 mW pump power with MoS_2 inside cavity. The laser operates with peak wavelength of 1560.2 nm and 5.9 nm of 3 dB spectral bandwidth. A stable pulse train of RFL is generated with an increasing repetition rate as the function of pump power is varied from 395 to 422 mW. It is observed that there are two peaks wavelength appeared which is probably due to the mode competition inside the ring cavity.

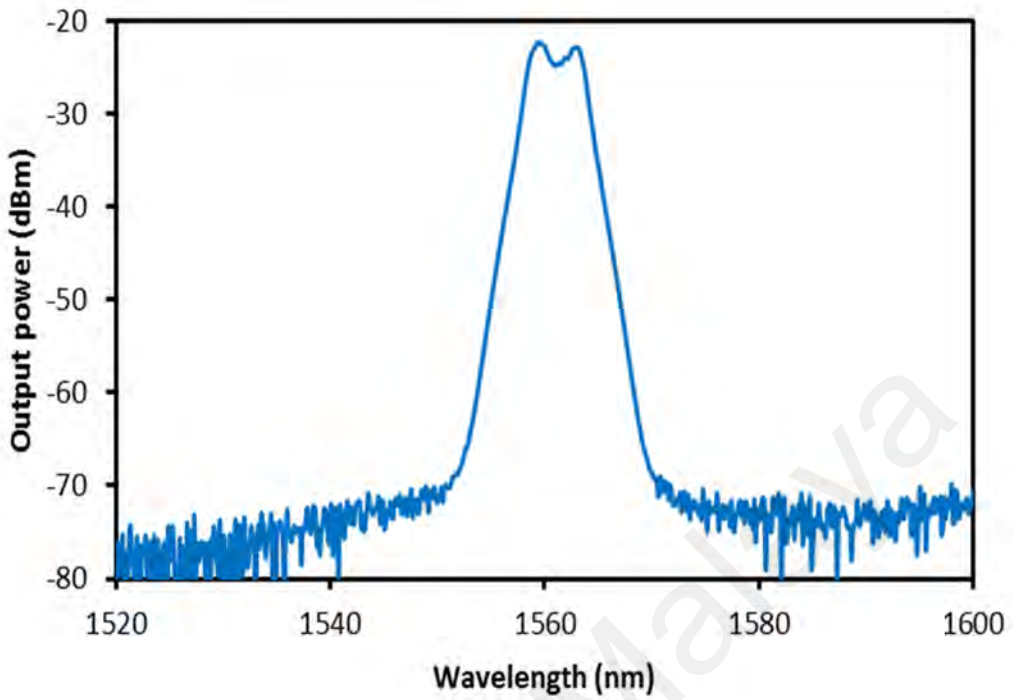

Figure 3.8: Optical spectra of RFL at pump power of 422 mW.

Figure 3.9 depicted the pulse train for typical laser output at pump power of 422 mW. It is indicated that the pulse train has the period of 7.27 μs without any chirp appeared, corresponding to the 137.4 kHz of repetition rate. In order to ensure that the MoS_2 SA was responsible in the generation of Q-switching pulse laser, the fiber ferrule filled with MoS_2 was substituted with another clean fiber ferrule. In this situation, there is no Q-switching pulse appeared on the OSC which verified the generated Q-switching operation was contributed by MoS_2 SA.

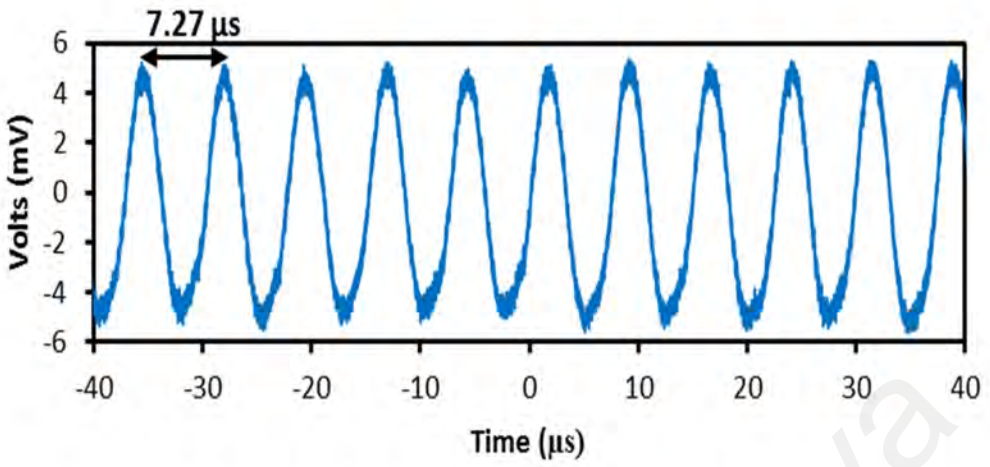

Figure 3.9: Typical oscilloscope trace under pump power of 422 mW.

Figure 3.10 shows the Q-switching repetition rate changed from 132.7 to 137.4 kHz as the input pump power is tuned from 395 to 422 mW. Meanwhile, the pulse width decreased from 3.35 to 3.03 µs. We also investigated the single-pulse energy and the output power at several pump powers. The plotted result in Figure 3.11 indicates that the pulse energy and output power is increased almost linearly with the rises of pump power. It is observed that the highest average output power is 7.46 mW with 2.65 % of efficiency. By deploying a higher nonlinearity gain media, the efficiency value could be improved and the total cavity length can be shortened. The maximum pulse energy of 54.3 nJ is achieved at the highest pump power of 422 mW.

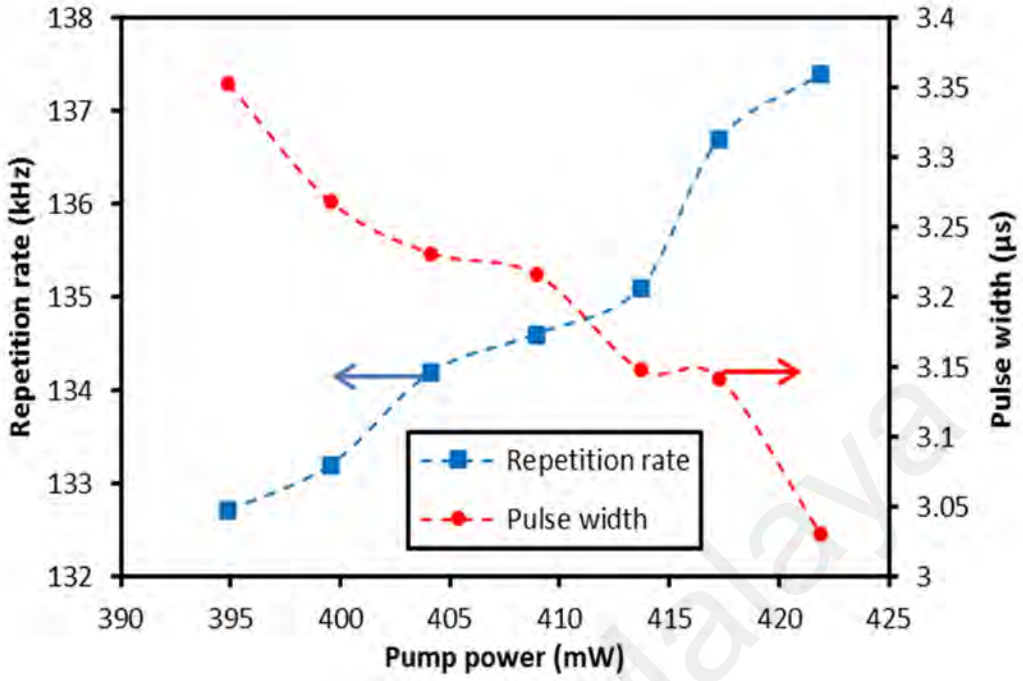

Figure 3.10: Repetition rate and pulse width variation with the increasing pump power.

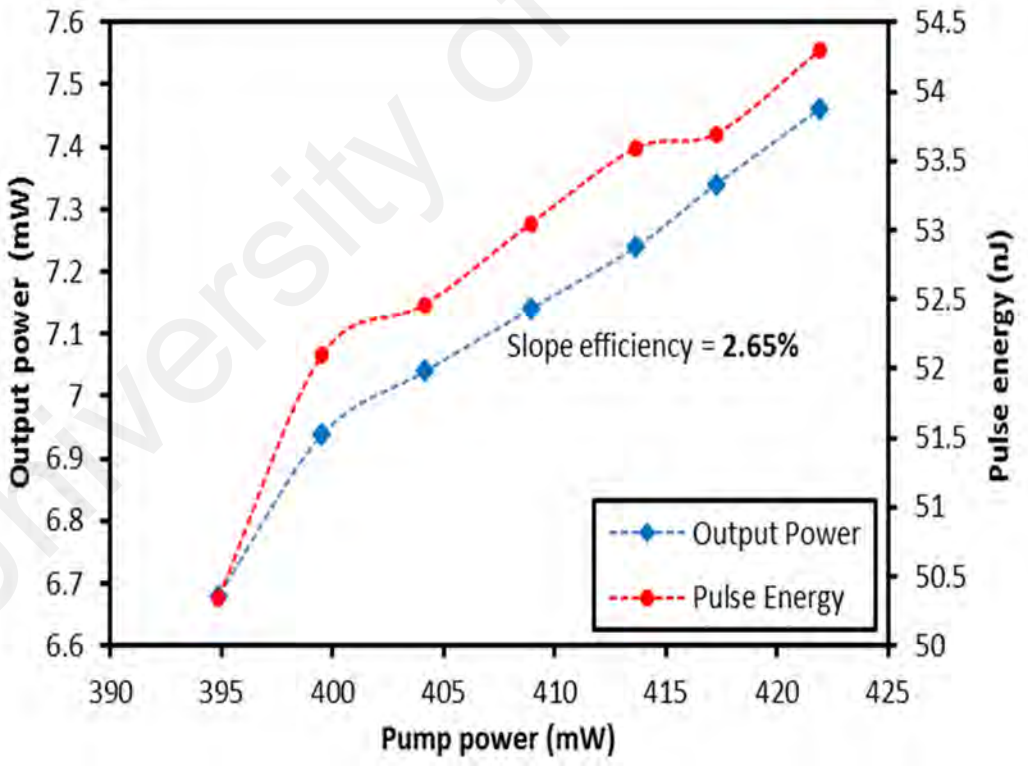

Figure 3.11: Output power and pulse energy against the pump powers.

The RF spectrum of Q-switching at pump power of 395 mW is shown in Figure 3.12. RF spectrum is a significant parameter that can verify and characterize the stability of the pulse. As illustrated in the figure, the fundamental repetition rate of the laser is obtained achieved at 132.7 kHz with an OSNR of 42 dB indicating the stability of the Q-switching pulse. Agree to Fourier transform, the peak of fundamental repetition rate gradually decrease until 3rd harmonic, and disappears. From this experiment, we confirmed that there is no mode-beating frequency presence. The generated pulse could be enhanced by optimizing the design of the laser cavity and the MoS_2 SA parameters such as insertion loss and modulation depth.

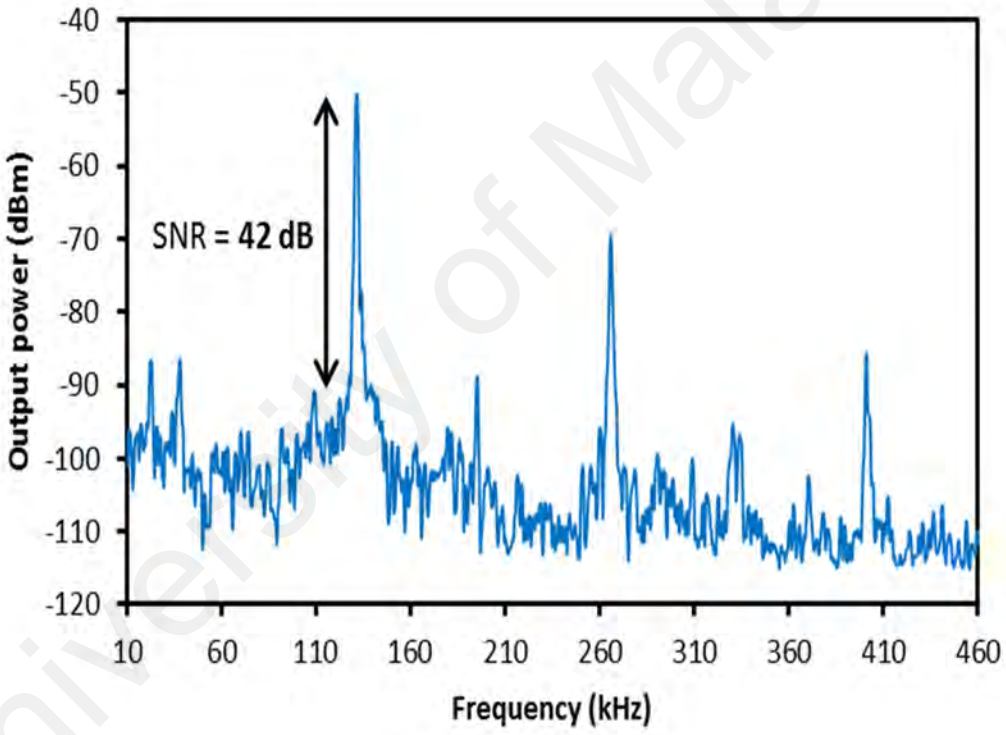

Figure 3.12: RF spectrum measured at pump power of 395 mW.

3.5 Summary

In conclusion, a passive Q-switched RFL using a MoS_2 as a SA is successfully demonstrated. The SA was prepared by depositing a mechanically exfoliated MoS_2 film onto the end face of fiber ferrule before it is connected with another clean ferrule using an optical adapter. By incorporating MoS_2 inside cavity, Q-switching pulse train is generated and operated at 1560.2 nm. By raising the pump power into cavity from 395 to 422 mW, the repetition rate varies from 132.7 to 137.4 kHz whereas the pulse width exhibited a decreasing trend from 3.35 to 3.03 μs. At the maximum pump power of 422 mW, the maximum pulse energy of 54.3 nJ is obtained. These results proved that the MoS_2 film is as effective for Q-switched pulsed laser applications.

CHAPTER 4: PASSIVELY Q-SWITCHED RAMAN FIBER LASER INCORPORATING TiO_2 AS SATURABLE ABSORBER

4.1 Introduction

Raman fiber lasers (RFLs) have attracted a great interest in recent years especially for operation at wavelengths that are difficult to achieve directly with ordinary gain media. They are developed based on stimulated Raman scattering (SRS) effect. In the previous chapter, a Q-switched RFL was demonstrated by using MoS_2 as a SA.

On the other hand, another interesting 2D transition metal oxides (TMOs) material which is Titanium (IV) oxide (TiO_2) has been utilized as saturable absorber for pulse laser generation. It has a low electrical resistivity (Martev, 2000) and offers high efficiency as a diffusion barrier against the interdiffusion of silica and aluminium. The conductive TiO_2 that could be utilized as a thin film material for microelectronic layered structures applications have also been reported. This saturable absorption ability is due to the Pauli-blocking principle. Recovery time is an important parameter to determine the Q-switching ability of saturable absorber which is around picosecond (ps). The recovery time of TiO_2 polymer film is ~ 1.5 ps. (Ahmad et al., 2016; Elim et al., 2003) the spectral absorption of TiO_2 can covers up to near-infrared (NIR) region although the band gap of TiO_2 is ~3.2 eV (Nambara et al., 2007; Reddy et al., 2003).

Of late, many investigations on TiO_2 optical properties such as the light absorption have been conducted. For instance the light absorption properties of blue titanium sub-oxide nanoparticles was investigated by (Wang et al., 2005). On the other hand, Polyvinyl alcohol (PVA) has been intensively used in many applications because of its capability to form film and favourable physical properties such as good chemical resistance, biocompatibility and hydrophilicity (Lopez et al., 2001).

As a 2D material, TiO_2 sheets can be easily exfoliated mechanically or chemically due to its strong in-plane bonding and weak van der Waals coupling between layers. In this chapter, a passively Q-switched RFL is demonstrated using a TiO_2 embedded in PVA as a Q-switcher. Stable pulsing with the repetition rate tunable from 131.4 to 142.5 kHz, the highest energy of 5.81 nJ and the smallest pulsewidth of 2.97 μs is obtained in a 8 km Q-switched resonator.

4.2 Fabrication and Characterization of TiO_2

TiO_2 solution is prepared by desolving a commercial anatase TiO_2 powder in distilled water with a help of 1 % sodium dodecyl sulphate (SDS) solvent. The TiO_2 powder has diameter of less than 45 μm and 99 % pure. To ensure that the TiO_2 material is dispersed homogeneously, the mixture is stirred for 5 minutes. TiO_2 solution was centrifuged for 15 minutes at 3000 rpm and the supernatant which contains TiO_2 suspension in the solution was collected for use. The dispersed TiO_2 solution was then added to a solution of the polymer. The polymer solution was obtained by mixing 1 g of PVA powders with 120 ml deionized water (DI). The mixture is stirred at 90 ^oC until the polymer was fully dispersed. Then, the polymer solutions were cooled down to room temperature. The TiO_2 and PVA mixture was mixed well through a centrifuging process to form a composite precursor solution. The precursor solution was poured onto a glass petri dish and heated in a vacuum oven for about 2 days to create a free standing film.The film obtained has an absorption of around 3 dB at 1550 nm with thickness of around 30 μm.

Figure 4.1(a) shows how the film was transferred onto a fiber ferrule. We also conducted Raman spectroscopy on the fabricated TiO_2 film sample to verify the presence of TiO_2 material. Figure 4.1(b) exhibits the Raman spectrum recorded by a spectrometer when a 514 nm beam of a Argon ion laser is radiated on the film for 10 ms with 50 mW of exposure

power. The sample shows five different Raman peaks at approximately 145, 198, 399, 516, and 640 cm^{-1}, which corresponds to the first E_g, second E_g, B_{1g}, A_{1g}, and third E_g band, respectively. High peak intensity at 145 cm^{-1} confirms this TiO_2 is only observed in the Raman spectrum of anatase crystalline structure. By performing a balance twin-detector measurement, the modulation depth of the film is measured to be around 33 %. A stable self-constructed passively mode-locked fiber laser (operating wavelength at 1560 nm with 980 fs of pulsewidth and 21.8 MHz of repetition rate) is utilized as the input pulse source.

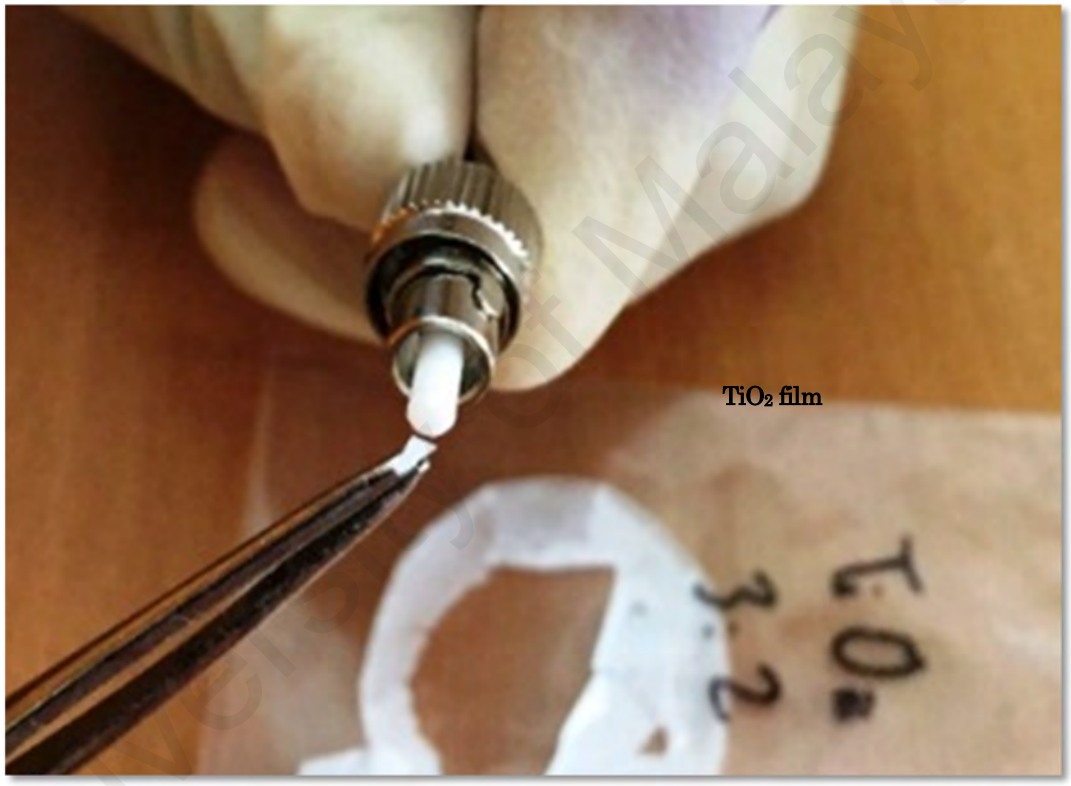

Figure 4.1(a): Image of fabricated TiO_2 film.

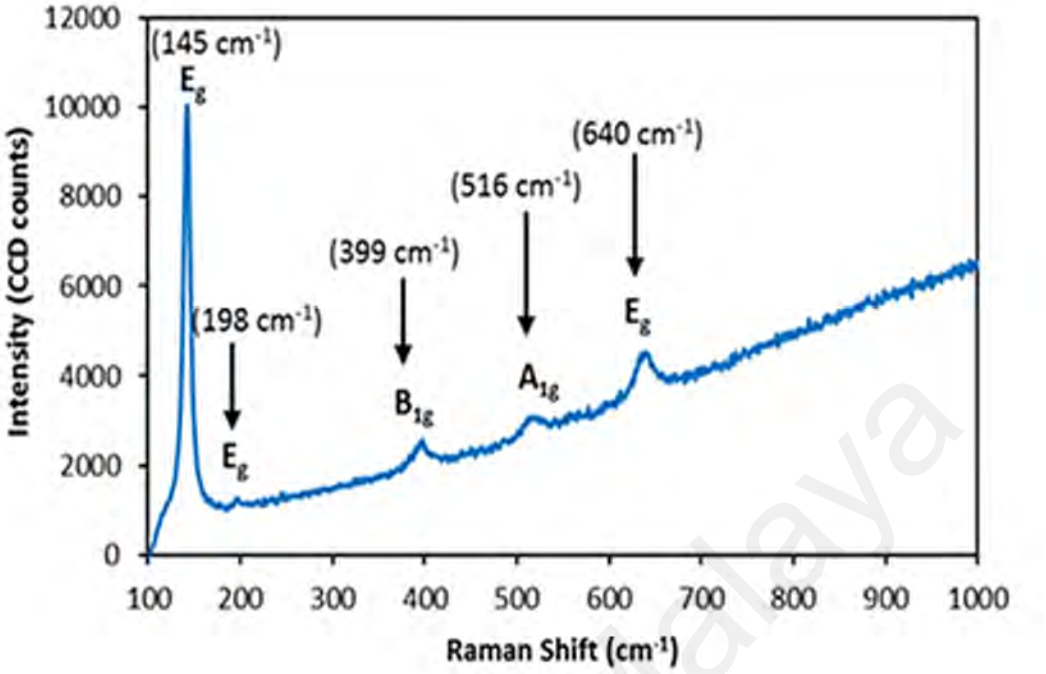

Figure 4.1(b): Raman spectrum of the fabricated TiO_2 film.

4.3 Experimental Setup for the Q-switched Raman Fiber Laser

Figure 4.2 shows the schematic diagram of the passively Q-switched RFL employing TiO_2 film as SA. A 7.7 km long of DCF with 584 ps/nm*km of dispersion work as a nonlinear gain media was directly pumped by a 1455 nm of Raman pump through a 1455/1550 nm WDM. The TiO_2 film was employed into the ring cavity by sandwiching a small portion of the TiO_2 film between two fibers ferrules via optical adapter adhered with index matching gel act as a passive Q-switcher. The isolator (ISO) is located inside cavity to ensure the unidirectional light operation. A 5/95 fiber coupler was used into the cavity after the SA with the 5 % port of the fiber coupler became output laser for spectrum and temporal characteristics. The spectral characteristic was measured using an OSA with a 0.02 nm of wavelength resolution while a 500 MHz OSC and a 7.8 GHz radio-frequency (RF) spectrum analyzer via a 1.2 GHz photo detector is used to measure the temporal diagnostics. The total length of the ring laser cavity is estimated about 8 km.

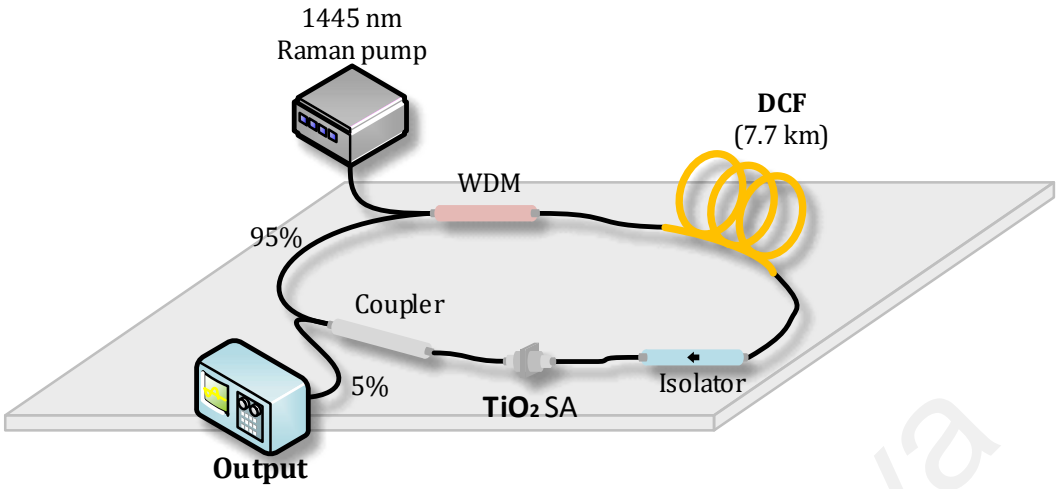

Figure 4.2: Schematic diagram of the proposed Q-switched RFL in a ring cavity.

4.4 Performance of Q-switched Raman Fiber Laser with TiO_2

Figure 4.3 compares the optical spectra of the RFL with and without the TiO_2 film based SA inside the cavity. In the experiment, the pump power of 1455 nm is fixed at 431 mW. It is obtained that the laser operates at peak wavelengths of 1558.5 nm and 1562.8 nm with and without the SA, respectively. It is observed that the peak wavelength shifts to a shorter wavelength when the TiO_2 film is inserted inside the cavity due to the increased cavity loss and it is shifted to shorter wavelength to compensate the losses. It is also observed that the generated spectrum is slightly broadened due to the TiO_2 enhances the nonlinear effect inside the cavity. The RFL generate a stable pulse train as the pump power is enhanced from 398 to 431 mW. Figure 4.4 represents the typical pulse train of the laser Q-switched at three distinct pump powers. The repetition rate almost linearly increased as the pump power is raised. At the highest pump power of 431 mW, the pulse train indicates the period of 7.12 μs without any noticeable timing jitter, corresponds to a pulse repetition rate of 142.5 kHz. To confirm the Q-switched pulse laser generation with the presence of TiO_2, the fiber ferrule with TiO_2 film was substituted with a clean fiber ferrule. It is observed that there is no Q-switching pulse appeared on the OSC at any pump powers, indicates that the Q-switching pulse has been contributed by TiO_2 SA.

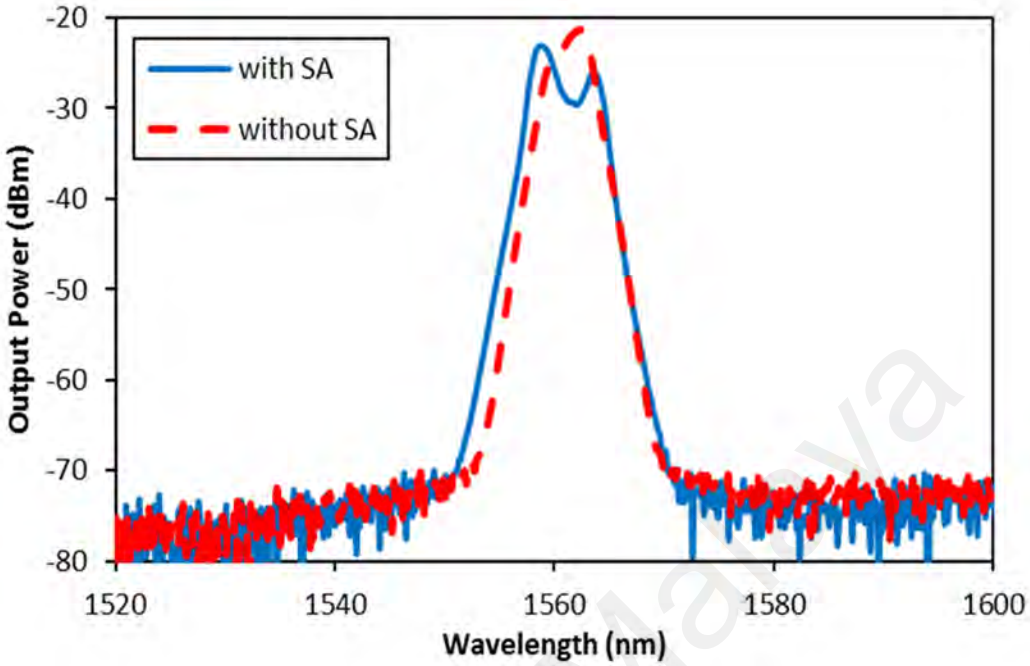

Figure 4.3: Optical spectra of RFL at pump power of 431 mW.

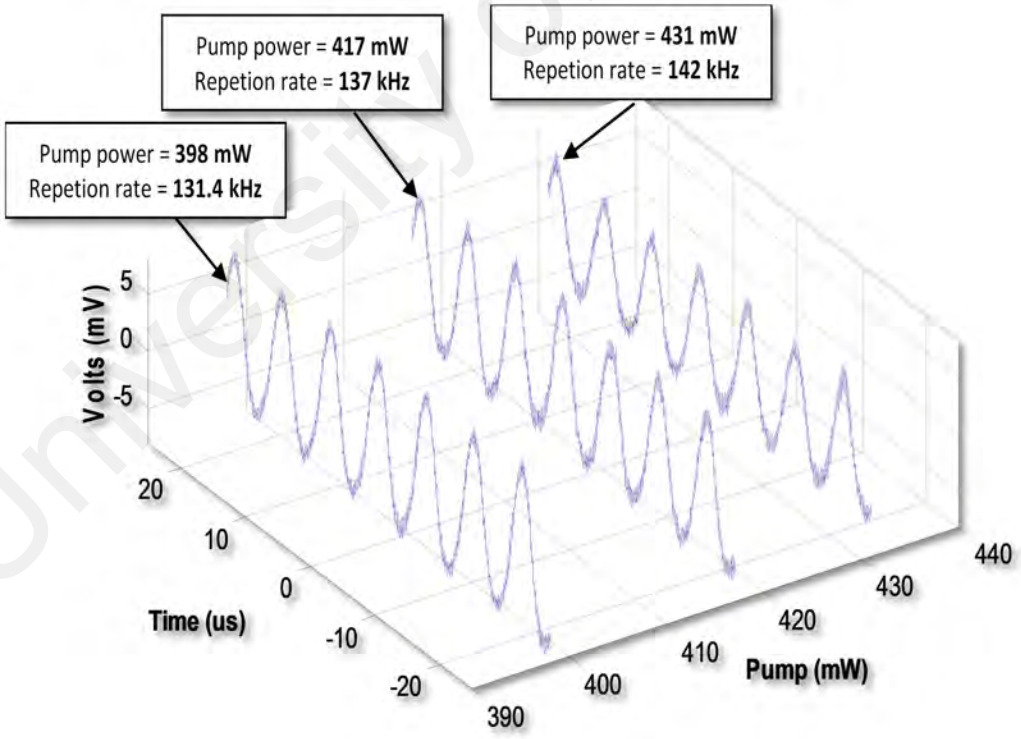

Figure 4.4: Typical oscilloscope trace under different pump power between 398 to 431 mW.

The plotted results in Figure 4.5 indicate that the repetition rate monotically increases from 131.4 to 142.5 kHz as the pump power is varied from 398 to 431 mW. On the other hand the pulse width decreased from 3.32 to 2.97 µs. It is noted that, by shortening the laser cavity length, the pulse width could be reduced more. The pulse energy and the output power of the laser are also studied at different pump power. Figure 4.6 showing that the output power almost linearly increased by raising pump power up to the pump power of 431 mW. The highest output power of the Q-switched laser is about 0.826 mW with the fiber efficiency is measured to be around 0.03 %. The laser efficiency value is rather low because of the cavity parameters were not optimized and high cavity loss inside cavity. From the plotted figure, it can be observed that the pulse energy fluctuates with the highest pulse energy of 5.81 nJ is obtained at 427 mW of pump power.

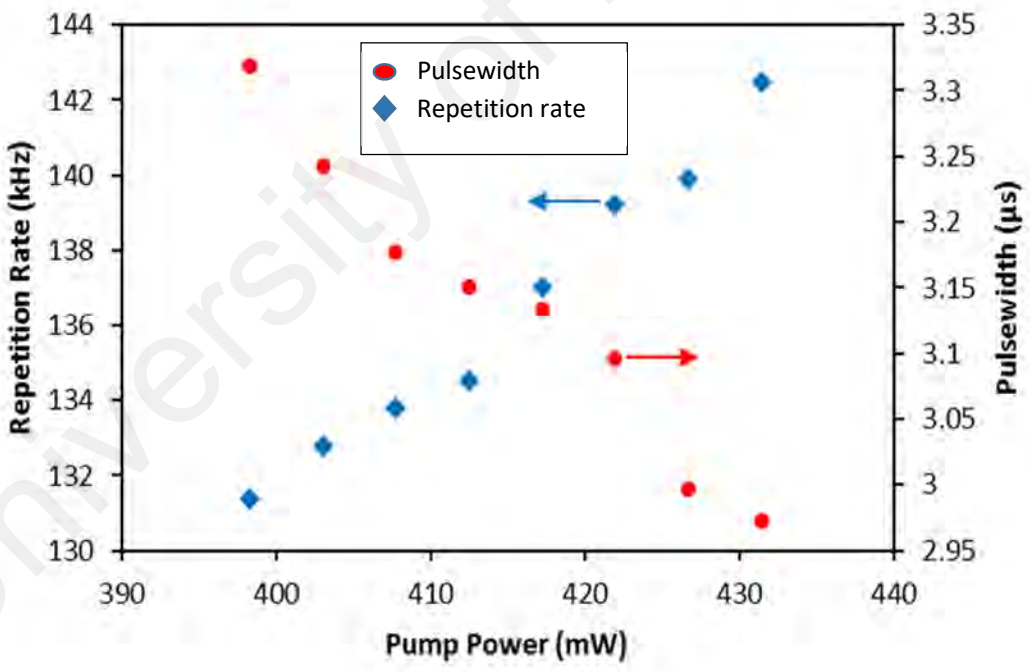

Figure 4.5: Repetition rate and pulse width variation with the increasing pump power.

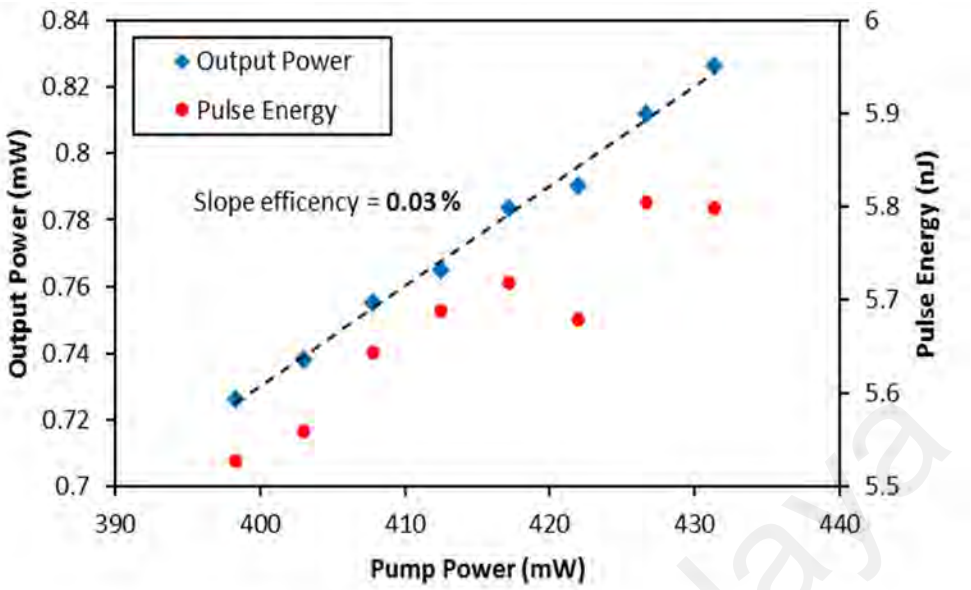

Figure 4.6: Output power and pulsed energy against the pump power.

The RF spectrum of Q-switching at pump power of 431 mW is shown in Figure 4.7. As shown in the figure, the fundamental repetition rate of the laser is 142.5 kHz which agrees with the pulse period of 7.12 μs .The SNR of the RF spectrum is observed at 37 dB, showing the stability of the Q-switching operation. Throughout the experiment, we can verify no mode-beating frequency presence. The Q-switching performance could be improved further by optimizing the cavity design and the parameters of TiO_2 SA.

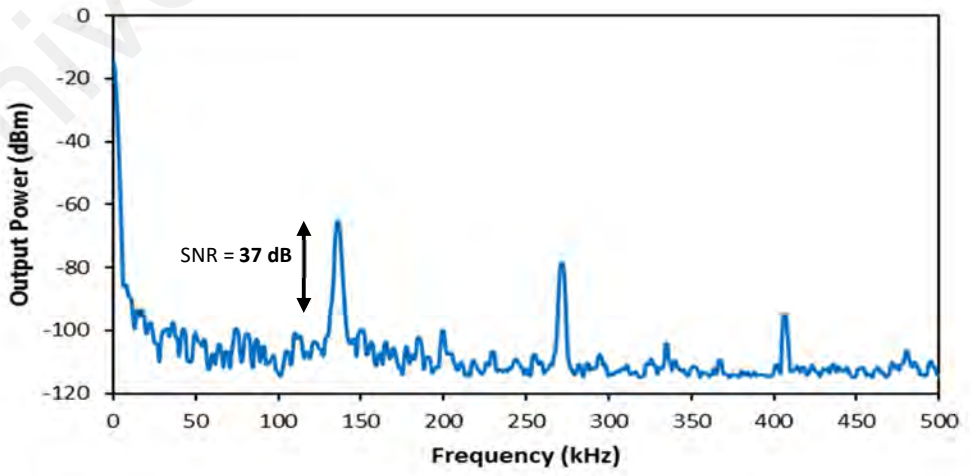

Figure 4.7: RF spectrum measured at pump power of 431 mW.

4.5 Summary

A Q-switched RFL has been successfully demonstrated using a TiO_2 film as a passive SA. The TiO_2 film was prepared by mixing the dispersed TiO_2 suspension into a PVA solution to form a precursor which is then transformed into a thin film through a drying process. It is placed between two fiber ferrules via an optical adapter to produce a fiber-compatible SA, which is then located inside RFL cavity to generate a Q-switched pulses at wavelength of 1558.5 nm. The repetition rate rises from 131.4 to 142.5 kHz and the pulse width decreased from 3.32 to 2.97 μs as the pump power is increased from 398 to 431 mW. The maximum output pulse energy of 5.81 nJ is achieved at pump power of 427 mW. These results verified that TiO_2 film can be utilized as an effective SA for pulsed laser applications.

CHAPTER 5: CONCLUSIONS AND FUTURE WORKS

5.1 Conclusions

In this study, all objectives have been achieved. The characterization of Raman fiber laser was conducted and passively Q-switching Raman fiber laser by incorporating different type of 2D materials as saturable absorber, Titanium dioxide (TiO_2) and Molybdenum disulfide (MoS_2) was successfully demonstrated.

In this contribution, MoS_2 and TiO_2 have been employed as saturable absorber in a fiber ring cavity for passively Q-switched Raman fiber laser generation operating in C-band regime for the first time. The advantages of the proposed SA are because of their remarkable nonlinear, electronic and optical characteristics. The SA is then integrated into ring cavity for microsecond pulse generation. Based on our experiment, both SA has great capability and reliability to generated Q-switched pulses with high peak power, short pulse duration and wide repetition rate range. By increasing the pump power from the threshold power, the repetition rate and pulse energy increase whereas the pulse width reduces. This performance indicates that the MoS_2 and TiO_2 SA also possess excellent ability for Q-switched pulse generation and hold great potential for ultrafast fiber laser applications.

5.2 Future Works

There is several future works that can be focused on the following topics:

1- Carry out the experiment by using different types of high nonlinear fiber such as single mode fiber (SMF), dispersion shifted fiber (DCF) and non-zero dispersion-shifted fiber (NZDSF) to generate mode-lock pulse laser operation.

2- Conduct an experiment by placing longer high nonlinear fiber in the optical cavity and observe the generated pulses.

3- Demonstrate an experiment by utilizing different types of 2D material as saturable absorber to explore and investigate their performances in generating pulse laser.

REFERENCES

Ahmad, H., Ismail, M. A., Suthaskumar, M., Tiu, Z. C., Harun, S. W., Zulkifli, M. Z., & Sivaraj, S. (2016). S-band Q-switched fiber laser using molybdenum disulfide (MoS2) saturable absorber. *Laser Physics Letters*, *13*(3), 035103.

Ahmad, H., Reduan, S. A., Ali, Z. A., Ismail, M. A., Ruslan, N. E., Lee, C. S. J., & Harun, S. W. (2016). C-Band Q-Switched Fiber Laser Using Titanium Dioxide (TiO2) As Saturable Absorber. *IEEE Photonics Journal*, *8*(1), 1-7.

André, P. S., Pinto, A. N., Teixeira, A. L. J., Neto, B., Stevan Jr, S., Sperti, D., ... & Rocha, A. (2008). New challenges in Raman amplification for fiber communication systems. New York: Nova Science Publisher.

Bai, X., Mou, C., Xu, L., Wang, S., Pu, S., & Zeng, X. (2016). Passively Q-switched erbium-doped fiber laser using Fe3O4-nanoparticle saturable absorber. *Applied Physics Express*, *9*(4), 042701.

Bao-Q, Y., Zheng, C., Xiao-M, D., Ying-J, S., Ji, W., & Yan-Q, D. (2014). A graphene-based passively Q-switched Ho: YAG laser. *Chinese Physics Letters*, *31*(7), 074204.

Bonaccorso, F., Sun, Z., Hasan, T., & Ferrari, A. C. (2011, October). Graphene composites for ultrafast photonics. In *Microopics Conference (MOC), 2011 17th* (pp. 1-4). IEEE.

Bonaccorso, F., Sun, Z., Hasan, T., & Ferrari, A. C. (2010). Graphene photonics and optoelectronics. *Nature Photonics*, *4*(9), 611-622.

Bromage, J. (2004). Raman amplification for fiber communications systems. *Journal of Lightwave Technology*, *22*(1), 79-93.

Chamorovskiy, A. Y., Marakulin, A. V., Kurkov, A. S., Leinonen, T., & Okhotnikov, O. G. (2012). High-repetition-rate Q-switched holmium fiber laser. *IEEE Photonics Journal*, *4*(3), 679-683.

Chen, B., Zhang, X., Wu, K., Wang, H., Wang, J., & Chen, J. (2015). Q-switched fiber laser based on transition metal dichalcogenides MoS2, MoSe2, WS2, and WSe2. *Optics Express*, *23*(20), 26723-26737.

Clowes, J. (2008). Next generation light sources for biomedical applications. *Optik & Photonik*, *3*(1), 36-38.

Dong, B., Hao, J., Hu, J., & Liaw, C. Y. (2010). Wide pulse-repetition-rate range tunable nanotube Q-switched low threshold erbium-doped fiber laser. *IEEE Photonics Technology Letters*, *22*(24), 1853-1855.

Elim, H. I., Ji, W., Yuwono, A. H., Xue, J. M., & Wang, J. (2003). Ultrafast optical nonlinearity in poly (methylmethacrylate)-TiO2 nanocomposites. *Applied Physics Letters*, *82*(16), 2691-2693.

Fermann, M. E., & Hartl, I. (2013). Ultrafast fibre lasers. *Nature Photonics*, *7*(11), 868-874.

Garmire, E. (2000). Resonant optical nonlinearities in semiconductors. *IEEE Journal of Selected Topics in Quantum Electronics*, *6*(6), 1094-1110.

Haiml, M., Grange, R., & Keller, U. (2004). Optical characterization of semiconductor saturable absorbers. *Applied Physics B: Lasers and Optics*, *79*(3), 331-339.

Harun, S. W., Ahmad, H., Ismail, M. A., & Ahmad, F. (2013, April). Q-switched and soliton pulses generation based on carbon nanotubes saturable absorber. In *Electronics, Communications and Photonics Conference (SIECPC), 2013 Saudi International* (pp. 1-4). IEEE.

Harun, S. W., Ismail, M. A., Ahmad, F., Ismail, M. F., Nor, R. M., Zulkepely, N. R., & Ahmad, H. (2012). A Q-switched erbium-doped fiber laser with a carbon nanotube based saturable absorber. *Chinese Physics Letters*, *29*(11), 114202.

Headley, C., & Agrawal, G. (Eds.). (2005). *Raman amplification in fiber optical communication systems*. Academic press.

Henderson, S. W., Suni, P. J., Hale, C. P., Hannon, S. M., Magee, J. R., Bruns, D. L., & Yuen, E. H. (1993). Coherent laser radar at 2 mu m using solid-state lasers. *IEEE Transactions on Geoscience and Remote Sensing*, *31*(1), 4-15.

Hisamuddin, N., Zakaria, U. N., Zulkifli, M. Z., Latiff, A. A., Ahmad, H., & Harun, S. W. (2016). Q-Switched Raman Fiber Laser with Molybdenum Disulfide-Based Passive Saturable Absorber. *Chinese Physics Letters*, *33*(7), 074208.

Hudson, D. D. (2009). *Mode-locked fiber lasers: Development and application* (Doctoral dissertation, University of Colorado at Boulder).

Islam, M. (2003). Raman Amplifiers for Telecommunications 1, Physical Principles and Raman Amplifiers for Telecommunications 2, Sub-Systems and Systems. *Springer Series in Optical Sciences (Springer-Verlag, 2003)*.

Jiang, T., Yin, K., Zheng, X., Yu, H., & Cheng, X. A. (2015). Black phosphorus as a new broadband saturable absorber for infrared passively Q-switched fiber lasers. *arXiv preprint arXiv:1504.07341*.

Juhasz, T., Loesel, F. H., Kurtz, R. M., Horvath, C., Bille, J. F., & Mourou, G. (1999). Corneal refractive surgery with femtosecond lasers. *IEEE Journal of Selected Topics in Quantum Electronics*, *5*(4), 902-910.

Jun-L, W., Xue-L, W., Bo-R, H., Yong-G, W., Jiang-F, Z., & Zhi-Y, W. (2015). High-Pulse-Energy All-Normal-Dispersion Yb-Doped Fiber Laser Based on Nonlinear Polarization Evolution. *Chinese Physics Letters*, *32*(11), 114202.

Kang, Y. (2002). Calculations and measurements of Raman gain coefficients of different fiber types (Master dissertation, Virginia Polytechnic Institute and State University).

Kashiwagi, K., & Yamashita, S. (2010). Optical deposition of carbon nanotubes for fiber-based device fabrication. In *Frontiers in Guided Wave Optics and Optoelectronics*. InTech.

Keller, U., Weingarten, K. J., Kartner, F. X., Kopf, D., Braun, B., Jung, I. D., ... & Der Au, J. A. (1996). Semiconductor saturable absorber mirrors (SESAM's) for femtosecond to nanosecond pulse generation in solid-state lasers. *IEEE Journal of Selected Topics in Quantum Electronics*, *2*(3), 435-453.

Khazaeinezhad, R., Nazari, T., Jeong, H., Park, K. J., Kim, B. Y., Yeom, D. I., & Oh, K. (2015). Passive Q-switching of an all-fiber laser using WS 2-deposited optical fiber taper. *IEEE Photonics Journal*, *7*(5), 1-7.

Kim, K., Guo, Z., Li, J. J., & Kumar, S. (2003, March). Radiation heat transfer in tissue welding and soldering with ultrafast lasers. In *Bioengineering Conference, 2003 IEEE 29th Annual, Proceedings of* (pp. 185-186). IEEE.

Kj, Rasmus. (2008). Raman amplification in optical communication systems (Doctoral dissertation, Technical University of Denmark).

Knox, W. H. (2000). Ultrafast technology in telecommunications. *IEEE Journal of Selected Topics in Quantum Electronics*, *6*(6), 1273-1278.

Koester, C. J., & Snitzer, E. (1964). Amplification in a fiber laser. *Applied Optics*, *3*(10), 1182-1186.

Krause, M., Cierullies, S., Renner, H., & Brinkmeyer, E. (2003). Design of widely tunable Raman fibre lasers supported by switchable FBG resonators. *Electronics Letters*, *39*(25), 1.

Kuang, Q., Zhan, L., Gu, Z., & Wang, Z. (2015). High-energy passively mode-locked Raman fiber laser pumped by a CW multimode laser. *Journal of Lightwave Technology*, *33*(2), 391-395.

Kuc, A., Zibouche, N., & Heine, T. (2011). Influence of quantum confinement on the electronic structure of the transition metal sulfide TS2. *Physical Review B*, *83*(24), 245213.

Kurkov, A. S. (2011). Q-switched all-fiber lasers with saturable absorbers. *Laser Physics Letters*, *8*(5), 335.

López, D., Cendoya, I., Torres, F., Tejada, J., & Mijangos, C. (2001). Preparation and characterization of poly (vinyl alcohol)-based magnetic nanocomposites. 1. Thermal and mechanical properties. *Journal of Applied Polymer Science*, *82*(13), 3215-3222.

Li, D., Jussila, H., Karvonen, L., Ye, G., Lipsanen, H., Chen, X., & Sun, Z. (2015). Ultrafast pulse generation with black phosphorus. *arXiv preprint arXiv:1505.00480*.

Li, H., Zhang, Q., Yap, C. C. R., Tay, B. K., Edwin, T. H. T., Olivier, A., & Baillargeat, D. (2012). From bulk to monolayer MoS2: evolution of Raman scattering. *Advanced Functional Materials*, *22*(7), 1385-1390.

Limpert, J., Roser, F., Schreiber, T., & Tunnermann, A. (2006). High-power ultrafast fiber laser systems. *IEEE Journal of Selected Topics in Quantum Electronics*, *12*(2), 233-244.

Liu, X., Du, D., & Mourou, G. (1997). Laser ablation and micromachining with ultrashort laser pulses. *IEEE Journal of Quantum Electronics*, *33*(10), 1706-1716.

Liu, H. H., Chow, K. K., Yamashita, S., & Set, S. Y. (2013). Carbon-nanotube-based passively Q-switched fiber laser for high energy pulse generation. *Optics & Laser Technology*, *45*, 713-716.

Liu, J., Xu, J., & Wang, P. (2012). Graphene-based passively Q-switched 2 μm thulium-doped fiber laser. *Optics Communications*, *285*(24), 5319-5322.

Luo, L., & Chu, P. L. (1999). Passive Q-switched erbium-doped fibre laser with saturable absorber. *Optics Communications*, *161*(4), 257-263.

Luo, Z., Huang, Y., Weng, J., Cheng, H., Lin, Z., Xu, B., & Xu, H. (2013). 1.06 μm Q-switched ytterbium-doped fiber laser using few-layer topological insulator Bi2 Se3 as a saturable absorber. *Optics Express*, *21*(24), 29516-29522.

Luo, Z., Wu, D., Xu, B., Xu, H., Cai, Z., Peng, J., & Sun, Z. (2016). Two-dimensional material-based saturable absorbers: towards compact visible-wavelength all-fiber pulsed lasers. *Nanoscale*, *8*(2), 1066-1072.

Luo, Z. C., Liu, M., Guo, Z. N., Jiang, X. F., Luo, A. P., Zhao, C. J., & Zhang, H. (2015). Microfiber-based few-layer black phosphorus saturable absorber for ultra-fast fiber laser. *Optics Express*, *23*(15), 20030-20039.

Ma, J., Xie, G., Lv, P., Gao, W., Yuan, P., Qian, L., & Wang, J. (2014). Wavelength-versatile graphene-gold film saturable absorber mirror for ultra-broadband mode-locking of bulk lasers. *Scientific Reports*, *4*. https://doi.org/10.1103/PhysRevLett.7.444

Maas, D. J. H. C., Bellancourt, A. R., Hoffmann, M., Rudin, B., Barbarin, Y., Golling, M., & Keller, U. (2008). Growth parameter optimization for fast quantum dot SESAMs. *Optics Express*, *16*(23), 18646-18656.

Martev, I. N. (2000). Oxygen-ion-assisted deposition of TiO films. *Vacuum*, *58*(2), 327-334.

Martinez, A., Fuse, K., & Yamashita, S. (2011). Mechanical exfoliation of graphene for the passive mode-locking of fiber lasers. *Applied Physics Letters*, *99*(12), 121107.

Martinez, A., & Sun, Z. (2013). Nanotube and graphene saturable absorbers for fibre lasers. *Nature Photonics*, *7*(11), 842-845.

Mohd Zamani, Z. (2012). *Study of S-band optical amplifiers and its applications/Mohd Zamani Zulkifli* (Doctoral dissertation, University of Malaya).

Muhammad, F. D. (2014). *Graphene as saturable absorber for photonics applications/Farah Diana binti Muhammad* (Doctoral dissertation, University of Malaya).

Nair, R. R., Blake, P., Grigorenko, A. N., Novoselov, K. S., Booth, T. J., Stauber, T., & Geim, A. K. (2008). Fine structure constant defines visual transparency of graphene. *Science*, *320*(5881), 1308-1308.

Nambara, T., Yoshida, K., Miao, L., Tanemura, S., & Tanaka, N. (2007). Preparation of strain-included rutile titanium oxide thin films and influence of the strain upon optical properties. *Thin Solid Films*, *515*(5), 3096-3101.

Namiki, S., & Emori, Y. (2001). Ultrabroad-band Raman amplifiers pumped and gain-equalized by wavelength-division-multiplexed high-power laser diodes. *IEEE Journal of Selected Topics in Quantum Electronics*, *7*(1), 3-16.

Nicholson, J. W. (2003). Dispersion compensating Raman amplifiers with pump reflectors for increased efficiency. *Journal of Lightwave Technology*, *21*(8), 1758.

Wang, K., Wang, J., Fan, J., Lotya, M., O'Neill, A., Fox, D., & Zhang, H. (2013). Ultrafast saturable absorption of two-dimensional MoS2 nanosheets. *ACS Nano*, *7*(10), 9260-9267.

Pei-G, Y., Shuang-C, R., Yong-Q, Y., Chun-Y, G., Yuan, G., & Cheng-X, L. (2006). High power photonic crystal fibre Raman laser. *Chinese Physics Letters*, *23*(6), 1476.

Popa, D., Sun, Z., Hasan, T., Torrisi, F., Wang, F., & Ferrari, A. C. (2011). Graphene Q-switched, tunable fiber laser. *Applied Physics Letters*, *98*(7), 073106.

Qin, Z., Xie, G., Zhang, H., Zhao, C., Yuan, P., Wen, S., & Qian, L. (2015). Black phosphorus as saturable absorber for the Q-switched Er: ZBLAN fiber laser at 2.8 μm. *Optics Express*, *23*(19), 24713-24718.

Ravet, G., Fotiadi, A. A., Blondel, M., & Megret, P. (2004). Passive Q-switching in all-fibre Raman laser with distributed Rayleigh feedback. *Electronics Letters*, *40*(9), 528-529.

Reddy, K. M., Manorama, S. V., & Reddy, A. R. (2003). Bandgap studies on anatase titanium dioxide nanoparticles. *Materials Chemistry and Physics*, *78*(1), 239-245.

Rong-H, C., Ke-C, L., Yi-G, L., Hong-X, S., & Xiao-Y, D. (2003). Experimental and Numerical Analysis of a Two-Order Cascaded Raman Fibre Laser. *Chinese Physics Letters*, *20*(2), 234.

Saidin, N., Zen, D. I. M., Hamida, B. A., Khan, S., Ahmad, H., Dimyati, K., & Harun, S. W. (2013). A Q-switched thulium-doped fiber laser with a graphene thin film based saturable absorber. *Laser Physics*, *23*(11), 115102.

Saleh, Z. S., Anyi, C. L., Rahman, A. A., Ali, N. M., Harun, S. W., Manaf, M., & Arof, H. (2014). Q-switched erbium-doped fibre laser using graphene-based saturable absorber obtained by mechanical exfoliation. *Ukrainian Journal of Physical Optics*, 15(1), 24-29.

Schibli, T. R., Minoshima, K., Kataura, H., Itoga, E., Minami, N., Kazaoui, S., & Sakakibara, Y. (2005). Ultrashort pulse-generation by saturable absorber mirrors based on polymer-embedded carbon nanotubes. *Optics Express*, *13*(20), 8025-8031.

Schröder, J., Coen, S., Vanholsbeeck, F., & Sylvestre, T. (2006). Passively mode-locked Raman fiber laser with 100 GHz repetition rate. *Optics Letters*, *31*(23), 3489-3491.

Set, S. Y., Yaguchi, H., Tanaka, Y., & Jablonski, M. (2004). Ultrafast fiber pulsed lasers incorporating carbon nanotubes. *IEEE Journal of Selected Topics in Quantum Electronics*, *10*(1), 137-146.

Snitzer, E. (1961). Optical maser action of Nd+3 in a barium crown glass. *Physical Review Letters*, *7*(12), 444.

Sotor, J., Sobon, G., Macherzynski, W., Paletko, P., & Abramski, K. M. (2015). Black phosphorus saturable absorber for ultrashort pulse generation. *Applied Physics Letters*, *107*(5), 051108.

Tang, P., Zhang, X., Zhao, C., Wang, Y., Zhang, H., Shen, D., ... & Fan, D. (2013). Topological Insulator: Saturable Absorber for the Passive Q-Switching Operation of an in-Band Pumped 1645-nm Er: YAG Ceramic Laser. *IEEE Photonics Journal*, *5*(2), 1500707-1500707.

Tiu, Z. C., Zarei, A., Tan, S. J., Ahmad, H., & Harun, S. W. (2014). Q-Switching Pulse Generation with Thulium-Doped Fiber Saturable Absorber. *Chinese Physics Letters*, *31*(12), 124203.

Tongay, S., Varnoosfaderani, S. S., Appleton, B. R., Wu, J., & Hebard, A. F. (2012). Magnetic properties of MoS 2: Existence of ferromagnetism. *Applied Physics Letters*, *101*(12), 123105.

Wang, S., Yu, H., & Zhang, H. (2015). Band-gap modulation of two-dimensional saturable absorbers for solid-state lasers. *Photonics Research*, *3*(2), A10-A20.

Wang, R., Chien, H. C., Kumar, J., Kumar, N., Chiu, H. Y., & Zhao, H. (2013). Third-harmonic generation in ultrathin films of MoS2. *ACS Applied Materials & Interfaces*, *6*(1), 314-318.

Wang, Y., Qin, Y., Li, G., Cui, Z., & Zhang, Z. (2005). One-step synthesis and optical properties of blue titanium suboxide nanoparticles. *Journal of Crystal Growth*, *282*(3), 402-406.

Woodward, R. I., Howe, R. C. T., Hu, G., Torrisi, F., Zhang, M., Hasan, T., & Kelleher, E. J. R. (2015). Few-layer MoS 2 saturable absorbers for short-pulse laser technology: current status and future perspectives. *Photonics Research*, *3*(2), A30-A42.

Wu, K., Zhang, X., Wang, J., Li, X., & Chen, J. (2015). WS 2 as a saturable absorber for ultrafast photonic applications of mode-locked and Q-switched lasers. *Optics Express*, *23*(9), 11453-11461.

Yao, T., Harish, A. V., Sahu, J. K., & Nilsson, J. (2015). High-power continuous-wave directly-diode-pumped fiber Raman lasers. *Applied Sciences*, *5*(4), 1323-1336.

Yim, C., O'Brien, M., McEvoy, N., Winters, S., Mirza, I., Lunney, J. G., & Duesberg, G. S. (2014). Investigation of the optical properties of MoS2 thin films using spectroscopic ellipsometry. *Applied Physics Letters*, *104*(10), 103114.

Zhang, H., Lu, S. B., Zheng, J., Du, J., Wen, S. C., Tang, D. Y., & Loh, K. P. (2014). Molybdenum disulfide (MoS 2) as a broadband saturable absorber for ultra-fast photonics. *Optics Express*, *22*(6), 7249-7260.

Zhang, L. Q., Zhuo, Z., Wang, J. X., & Wang, Y. Z. (2012). Passively Q-switched fiber laser based on graphene saturable absorber. *Laser Physics*, *22*(2), 433-436.

Zhao, J., Wang, Y., Yan, P., Ruan, S., Tsang, Y., Zhang, G., & Li, H. (2014). An Ytterbium-doped fiber laser with dark and Q-switched pulse generation using graphene-oxide as saturable absorber. *Optics Communications*, *312*, 227-232.

LIST OF PUBLICATION AND PAPER PRESENTED

Journal

1) **Hisamuddin, N.**, Zakaria, U. N., Zulkifli, M. Z., Latiff, A. A., Ahmad, H., & Harun, S, W. (2016). Q-Switched Raman Fiber Laser with Molybdenum Disulfide-Based Passive Saturable Absorber. *Chinese Physics Letters, 33(7), 074208.*

Conference

1) **Hisamuddin, N.**, Ahmad, H., Zulkifli, M. Z., & Harun, S, W. (2016). S-band Half-Open Cavity Random Fiber Laser.*Proceedings of 4thInternational Science Postgraduate Conference 2016 (ISPC2016)*.Faculty of Science, Universiti Teknologi Malaysia

CHIN. PHYS. LETT. Vol. 33, No. 7 (2016) 074208

Q-Switched Raman Fiber Laser with Molybdenum Disulfide-Based Passive Saturable Absorber

N. Hisamuddin[1], U. N. Zakaria[2], M. Z. Zulkifli[1,3], A. A. Latiff[1], H. Ahmad[1], S. W. Harun[1,2]**

[1]*Photonics Research Center, University of Malaya, Kuala Lumpur 50603, Malaysia*
[2]*Department of Electrical Engineering, Faculty of Engineering, University of Malaya, Kuala Lumpur 50603, Malaysia*
[3]*Aston Institute of Photonics Technologies, Aston University, Birmingham B47ET, United Kingdom*

(Received 16 April 2016)

We demonstrate a Q-switched Raman fiber laser using molybdenum disulfide (MoS_2) as a saturable absorber (SA). The SA is assembled by depositing a mechanically exfoliated MoS_2 onto a fiber ferrule facet before it is matched with another clean ferrule via a connector. It is inserted in a Raman fiber laser cavity with a total cavity length of about 8 km to generate a Q-switching pulse train operating at 1560.2 nm. A 7.7-km-long dispersion compensating fiber with 584 ps·nm^{-1}km^{-1} of dispersion is used as a nonlinear gain medium. As the pump power is increased from 395 mW to 422 mW, the repetition rate of the Q-switching pulses can be increased from 132.7 to 137.4 kHz while the pulse width is concurrently decreased from 3.35 μs to 3.03 μs. The maximum pulse energy of 54.3 nJ is obtained at the maximum pump power of 422 mW. These results show that the mechanically exfoliated MoS_2 SA has a great potential to be used for pulse generation in Raman fiber laser systems.

PACS: 42.55.Wd, 42.55.Ye, 42.60.Gd DOI: 10.1088/0256-307X/33/7/074208

Stimulated Raman scattering (SRS) has been utilized to develop fiber lasers having wavelengths that are difficult to access directly with conventional gain media. In the SRS process, the amount of the Stokes frequency shift is intrinsically determined by the irradiated medium in which a quantum conversion increases proportionally with the complex part of the third-order nonlinear permittivity.[1] To date, various Raman fiber lasers (RFLs) have been fabricated and demonstrated by using germanosilicate or phosphosilicate glass fibers as Raman gain media. Most of the proposed lasers are operating with a cw mode with high output power. On the other hand, there is also growing interest in passively Q-switched fiber lasers due to their potential applications in LIDAR, remote sensing, communication and medicine.[2] Compared with the active technique, the passive approach is better in terms of simplicity, compactness, and flexibility of implementation.[3] The passive Q-switching generation can be realized by using either an artificial saturable absorber (nonlinear polarization rotation, nonlinear optical loop mirror) or real saturable absorber (SA) techniques.

To date, various real-SAs such as semiconductor SA mirrors (SESAMs), single wall carbon nanotubes (SWCNTs) and graphene saturable absorbers (SAs), have been exploited for realizing stable passive Q-switching. Compared with other passive techniques, graphene behaves as an excellent SA and its true potential in generating pulsed laser has been proved due to the combination of its unique optical and electronic properties.[4] The success of graphene has greatly encouraged scientific researchers to explore other graphene-like 2D nanomaterial for photonic applications.[5,6] Recently, topological insulators (TIs), a new class of nanomaterial characterized by an insulating bulk state and a gapless Dirac-type surface/edge,[7] have been attracting great interest in ultrafast photonics.[8] Taking advantage of the excellent saturable absorption of TIs, Luo *et al.* successfully experimentally demonstrated the generation of Q-switched pulses in ytterbium-doped fiber laser[9] and thulium-doped fiber laser[10] cavities operating at 1.06 μm and 2.0 μm, respectively.

Very recently, the saturable absorption of molybdenum disulfide (MoS_2), was also demonstrated by using the Z-scan technique at 800 nm.[11] By inserting the MoS_2 SA into an erbium-doped fiber laser (EDFL), a ∼710 fs pulse centered at 1569 nm wavelength with a repetition rate of 12.09 MHz was demonstrated.[12] In this Letter, we present a passively Q-switched RFL by a MoS_2-based SA using a 7.7-km-long dispersion compensating fiber (DCF) as the gain medium. The Q-switcher is assembled by depositing a mechanically exfoliated MoS_2 onto a fiber ferrule facet before it is matched with another clean ferrule via a connector. With the multilayer MoS_2-based SA, the compact all-fiber laser emits stable Q-switched pulses with threshold pump power, central wavelength, minimum pulse duration, and maximum repetition rate of 395 mW, 1560.2 nm, 3.03 μm and 137.4 kHz, respectively. To the best of our knowledge, a Q-switched RFL operating in any wavelength regions by using a passive SA has never been demonstrated before. Most of the previous works are focused on carbon nanotubes and graphene nanomaterials by using a doped fiber as

**Corresponding author. Email: swharun@um.edu.my